SOUTHERN PLAINS
TRANSPORTATION CENTER

Identifying Dust Emission "Hot Spots" in the Southern Plains Region of New Mexico, Oklahoma and Texas: Effect of Blowing Dust on Highway

JUNRAN LI, PH.D.
JEFFREY A. LEE, PH.D.
THOMAS E. GILL, PH.D.

SPTC14.1-39-F

Southern Plains Transportation Center
201 Stephenson Parkway, Suite 4200
The University of Oklahoma
Norman, Oklahoma 73019

DISCLAIMER

The contents of this report reflect the views of the authors, who are responsible for the facts and accuracy of the information presented herein. This document is disseminated under the sponsorship of the Department of Transportation University Transportation Centers Program, in the interest of information exchange. The U.S. Government assumes no liability for the contents or use thereof.

TECHNICAL REPORT DOCUMENTATION PAGE

1. REPORT NO.	2. GOVERNMENT ACCESSION NO.	3. RECIPIENTS CATALOG NO.
SPTC14.1-39-F		

4. TITLE AND SUBTITLE	5. REPORT DATE
Identifying Dust Emission "Hot Spots" in the Southern Plains Region of New Mexico, Oklahoma and Texas: Effect of Blowing Dust on Highway	December 30, 2017
	6. PERFORMING ORGANIZATION CODE
7. AUTHOR(S)	8. PERFORMING ORGANIZATION REPORT
Junran Li, Jeffrey A. Lee, Thomas E. Gill	
9. PERFORMING ORGANIZATION NAME AND ADDRESS	10. WORK UNIT NO.
The University of Tulsa, 800 Tucker Dr. Tulsa, OK 74104	
	11. CONTRACT OR GRANT NO. DTRT13-G-UTC36
12. SPONSORING AGENCY NAME AND ADDRESS	13. TYPE OF REPORT AND PERIOD COVERED
Southern Plains Transportation Center 201 Stephenson Pkwy, Suite 4200 The University of Oklahoma Norman, OK 73019	Final Report Jan 2015 – June 2017
	14. SPONSORING AGENCY CODE

15. SUPPLEMENTARY NOTES

University Transportation Center

16. ABSTRACT

Windblown dust poses a significant hazard to highway safety. Dust contributes to chain-reaction traffic accidents every year in the southwestern US, however, no known studies have specifically investigated this issue in New Mexico, Oklahoma, and Texas. In this study, we used remotely sensed and in situ observations of land cover, soil, and vegetation data to 1) identify the spatial and temporal distribution patterns of hotspots that may contribute dust blowing across highways in the southwestern United States, 2) identify the characteristics of the dust emission hotspots in relation to the distribution of highway, geomorphology, and land use, and 3) classify the hotspots for the potential of blowing dust production based upon field observations and dust emission modeling. A total of 620 total hotspots were identified for the period of 2010-2016 in the study area. Among all these dust emission sources, 234 (38%), 164 (27%), and 141 (23%) are located on cropland, shrubland, and grassland, respectively.

An analysis relating the distribution of dust sources and drought intensity in the study area showed that the dust points with highest drought intensities are concentrated on the Southern High Plains region, more specifically in a belt extending from the west to the south of Lubbock, Texas. We further investigated 55 of the dust emission sites, which are located <1km to adjacent highways. Field investigations and laboratory analysis showed that soils at these hotspot sites are dominated by sand and silt particles with threshold shear velocities ranging from 0.17-0.78 m s^{-1}. Dust emission modeling showed that 8 hotspot sites could produce annual emissions of >5.32 kg m^{-2}, yielding highly hazardous dust emissions to ground transportation with visibility <200 m. Results of location, timing, and magnitude of the dust production at the hotspots are critical information for highway authorities to make informed and timely management decisions when wind events strike.

17. KEY WORDS	18. DISTRIBUTION STATEMENT
Blowing dust, Highway safety, land use, remote sensing, GIS	No restrictions. This publication is available at www.sptc.org and from the NTIS.

19. SECURITY CLASSIF. (OF THIS REPORT)	20. SECURITY CLASSIF. (OF THIS PAGE)	21. NO. OF PAGES	22. PRICE
Unclassified	Unclassified	46	

SI* (MODERN METRIC) CONVERSION FACTORS

SYMBOL	WHEN YOU KNOW	MULTIPLY BY	TO FIND	SYMBOL
		LENGTH		
in	inches	25.4	millimeters	mm
ft	feet	0.305	meters	m
yd	yards	0.914	meters	m
mi	miles	1.61	kilometers	km
		AREA		
in^2	square inches	645.2	square millimeters	mm^2
ft^2	square feet	0.093	square meters	m^2
yd^2	square yard	0.836	square meters	m^2
ac	acres	0.405	hectares	ha
mi^2	square miles	2.59	square kilometers	km^2
		VOLUME		
fl	fluid ounces	29.57	milliliters	m
oz	gallons	3.785	liters	L
gal	cubic feet	0.028	cubic meters	L
ft^3	cubic yards	0.765	cubic meters	m^3
yd	NOTE: volumes greater than 1000 L shall be shown in m^3			m^3
		MASS		
oz	ounces	28.35	grams	g
lb	pounds	0.454	kilograms	kg
T	short tons (2000 lb)	0.907	megagrams (or "metric ton")	Mg (or "t")
		TEMPERATURE (exact degrees)		
^oF	Fahrenheit	5 (F-32)/9 or (F-32)/1.8	Celsius	^oC
		ILLUMINATION		
fc	foot-candles	10.76	lux	lx
fl	foot-Lamberts	3.426	candela/m^2	cd/m^2
		FORCE and PRESSURE or STRESS		
lbf	poundforce	4.45	newtons	N
lbf/in^2	poundforce per square inch	6.89	kilopascals	kPa

SYMBOL	WHEN YOU KNOW	MULTIPLY BY	TO FIND	SYMBOL
		LENGTH		
mm	millimeters	0.039	inches	in
m	meters	3.28	feet	ft
m	meters	1.09	yards	yd
km	kilometers	0.621	miles	mi
		AREA		
mm^2	square millimeters	0.0016	square inches	in^2
m^2	square meters	10.764	square feet	ft^2
m^2	square meters	1.195	square yards	yd^2
ha	hectares	2.47	acres	ac
km^2	square kilometers	0.386	square miles	mi^2
		VOLUME		
mL	milliliters	0.034	fluid ounces	fl oz
L	liters	0.264	gallons	gal
m^3	cubic meters	35.314	cubic feet	ft^3
m^3	cubic meters	1.307	cubic yards	yd^3
		MASS		
g	grams	0.035	ounces	oz
kg	kilograms	2.202	pounds	lb
Mg (or "t")	megagrams (or "metric ton")	1.103	short tons (2000 lb)	T
		TEMPERATURE (exact degrees)		
^oC	Celsius	1.8C+32	Fahrenheit	^oF
		ILLUMINATION		
lx	lux	0.0929	foot-candles	fc
cd/m^2	candela/m^2	0.2919	foot-Lamberts	fl
		FORCE and PRESSURE or STRESS		
N	newtons	0.225	poundforce	lbf
kPa	kilopascals	0.145	poundforce per square inch	lbf/in^2

Identifying Dust Emission "Hot Spots" in the Southern Plains Region of New Mexico, Oklahoma and Texas: Effect of Blowing Dust on Highway

Type of Report: Final

Date: December 2017

Junran Li, PH.D.
Jeffrey A. Lee, PH.D.
Thomas E. Gill, PH.D.
SPTC14.1-39-F

Southern Plains Transportation Center
201 Stephenson Pkwy, Suite 4200
The University of Oklahoma
Norman, Oklahoma 73019

ACKNOWLEDGEMENTS

Dr. Raed Aldouri, Director of the Regional Geospatial Service Center and Assistant Professor of Civil Engineering at University of Texas El Paso (UTEP), provided some assistance and advice to the project at no cost. Kagan Richard, Joe Collins (current affiliation: Texas A&M University, San Antonio), Iyasu Eibedingil, Julio Ceniceros, and Alexander Garcia, from the Environmental Science and Department of Geological Science at UTEP provided assistance to the project through the period in terms of field work and laboratory analysis. Tarek Kandakji from the Texas Tech University provided assistance on GIS and remote sensing analysis. At the University of Tulsa, John Blackwell III, Timothy Smith and Jose Van Dunem are acknowledged for their assistance in field work. John Tatarko (USDA-ARS, Fort Collins, CO) provided technical assistance on the dust emission modeling using WEPS.

TABLE OF CONTENTS

LIST OF FIGURES

LIST OF TABLES

EXECUTIVE SUMMARY

Windblown dust poses a significant hazard to highway safety. Dust contributes to chain-reaction traffic accidents every year in the southwestern US, however, no known studies have specifically investigated this issue in New Mexico, Oklahoma, and Texas. Remote sensing and field observations reveal that wind erosion in this region typically occurs in localized source areas, characterized as “hotspots”, while most of the landscape is not eroding. Currently, the spatial and temporal patterns of the hot spots and their relations to the occurrence of blowing dust to the highways are poorly understood. The lack of this critical information hinders highway managers’ ability to make informed and timely management decisions when wind events strike. Projected global changes, including changes in climate, land use, and land cover, will likely bring more frequent and extreme dust emissions to the southwestern US, including a majority of the Southern Plains, posing a serious threat to transportation safety in this region in the coming decades.

Excessive drought can also lead to an increase in sand and dust storms. Although drought has not shown any significant spatial expansion in the USA in the past 50 years, it has shown an increase in intensity and frequency [6]. Studies have shown that excessive drought was identified as one of the main factors that influenced the emergence of the Dust Bowl in this same region in the 1930’s. Therefore, it is of crucial importance to understand the relationship between dust storms and drought intensity in order to model and predict dust storm scenarios including those which have an effect on highway safety.

In this study, we used remotely sensed and *in situ* observations of land cover, soil, and vegetation data to 1) identify the spatial and temporal distribution patterns of hotspots that may contribute dust blowing across highways in the southwestern United States, 2) identify the characteristics of the dust emission hotspots in relation to the distribution of highway, geomorphology, and land use, and 3) classify the hotspots for the potential of blowing dust production based upon field observations and dust emission modeling. Collectively, the results from this study will contribute to the development of an integrated modeling and monitoring system to assist the management of the hazardous impacts of dust on highway safety.

In an area that includes the Southern High Plains and parts of dust-producing regions in the Chihuahuan Desert of New Mexico, north Texas and the intersection areas of Texas, Oklahoma, Kansas, and Colorado, a total of 620 total hotspots were identified for the period of 2010-2016. A majority of dust events associated with the dust sources occurred in spring (Feb-Mar) and winter (Nov-Dec), and the annual occurrence of dust events is also strongly affected by the annual precipitation. Among all these dust emission sources, 234 (38%), 164 (27%), and 141 (23%) are located on cropland, shrubland, and grassland, respectively. In terms of geomorphic surface, sand sheet and alluvial surfaces accounted for 48% and 25% of all the hotspots identified. The high emission ratios of barren land (land use) and ephemeral lakes (geomorphology) suggest that special attentions must be paid to those areas. Very similar patterns were also observed for dust sources for a time period extended back to 2001, in which a total of 1187 sources were identified.

Drought intensity analysis showed that there was a significant drought generally over the states of Texas, Oklahoma, and New Mexico region in the time periods 2001 – 2006 and 2011 – 2015. In connection to these trends there was also a high number of dust events after these droughts. An analysis relating the distribution of dust sources and drought intensity in the study area showed that the dust points with highest drought intensities are concentrated on the Southern High Plains region, more specifically in a belt extending from the west to the south of Lubbock, Texas.

By incorporating the distribution of highways, our study showed that a majority of the dust emission hotspots are located close to highways. We further investigated 55 of them, which are located <1km to adjacent highways and can be accessed via non-private roads. Field investigations and laboratory analysis showed that soils at these hotspot sites are dominated by sand and silt particles with threshold shear velocities ranging from 0.17-0.78 m s^{-1}, largely depending on the land use of the hotspot sites. Dust emission modeling showed that 8 hotspot sites could produce annual emissions of >5.32 kg m^{-2}, yielding highly hazardous dust emissions to ground transportation with visibility <200 m. Results of location, timing, and magnitude of the dust production at the hotspots are critical information for highway authorities to make informed and timely management decisions when wind events strike.

INTRODUCTION

The hazard of blowing dust to highway safety represents one of the significant impacts of aeolian processes on human welfare (Goudie, 2009; Baddock et al., 2013; Middleton, 2017). Goudie (2014) reported that dust-related fatal highway accidents happened in six states in the U.S. in 2012-2013. Earlier, Pauley et al. (1996) described a major incident in the San Joaquin Valley of California in 1991, where blowing dust led to 164 vehicles colliding and 168 dead or injured on U.S. Interstate Highway 5. Laity (2003) reported that dust mobilized from the Mojave River floodplain in California had caused fata highway accidents. In Arizona, Lader et al. (2016) reported that dust storms are the third largest cause of weather fatalities and dust-related incidents have killed 157 and injured 1324 people over the last 50 years. Nationwide in the U.S., Ashley and Black (2008) found that dust events caused by non-convective wind storms alone contributed to 62 deaths between 1980 and 2005. Dust representing a highway hazard is not restricted to barren desert environments: wind erosion of agricultural lands also can cause deadly accidents. For example, Deetz et al. (2016) described an incident where windblown sediment from a nearby potato field caused a multi-fatality motor vehicle wreck on a German autobahn.

In addition, dust blowing across roads has a significant economic cost manifested in additional highway maintenance, shutdown of roads and detouring of traffic which impact logistics and timely delivery of goods and services as well as disrupting the conveyance of people (Goudie and Middleton, 1992; Baddock et al., 2013). The effect of dust on vehicle traffic thus represents one of the most significant “off-site” costs of wind erosion (Pimental et al., 1995: Baddock et al., 2013). Despite the fact that blowing dust contributes to chain-reaction traffic incidents, delays in delivery, disrupts transportation schedules and causes and property damage every year in the U.S. and many other locations in the world, only a few studies have provided an in-depth analysis on the occurrence of such events, and little information is available to highway managers on the mitigation and management of this hazard.

From the “Dust Bowl” of the 1930s to the present, large areas of the North America’s Southern Great Plains, including northeastern New Mexico, western Oklahoma, western Texas, southeastern Colorado, and southwestern Kansas, have been noted for the occurrence of blowing dust (Lee and Tchakerican, 1995; Lee and Gill, 2015). The contiguous U.S. portion of the Chihuahuan Desert, extending from far eastern Arizona across southern New Mexico and far western Texas, is one of the most dust-prone regions in the Western Hemisphere (Prospero et al., 2002). Dust events in North American’s drylands may be driven by convective (mesoscale) or non-convective (synoptic-scale) windstorms (Novlan et al., 2007; Rivera Rivera et al., 2009). Remote sensing and field observations further revealed that dust in this region tends to emit from localized source areas associated with preferred land use, characterized as “hotspots”, while most of the landscape does not erode (Gillette, 1999; Mahowald et al., 2005; Lee et al., 2009; Rivera Rivera et al., 2010; Lee et al., 2012) (Fig. 1). In western Texas and eastern New Mexico, Lee et al. (2009) found that most of the observable dust plumes originated on anthropogenically disturbed lands, such as cultivated cropland, and plumes of dust that emanate from individual point sources eventually merge into a shield-shaped region of dust.

It is widely recognized that blowing dust affects highway safety due to the reduction of visibility. Observations made by motorists also revealed that most of the dust events that were hazardous to highway safety were emitted from lands adjacent to the highway (Day, 1993). Blowing dust is primarily composed of particles with diameter less than 50 μm and is produced as a result of the saltation of sand-sized particles (50-500 μm in diameter) sandblasting the surface (Goudie and Middleton, 2006). In a typical dust-related traffic incident on the highway, suspension of dust-sized particles may cause the deterioration of visibility whereas the near-surface transport and deposition of saltation-sized particles may reduce the traction on the road surface.

Excessive drought can also lead to an increase in sand and dust storms (Prospero and Lamb, 2003; Wu et al., 2013; Notaro et al., 2015). Although drought has not shown any significant spatial expansion in the USA in the past 50 years, it has shown an increase in intensity and frequency (Ganguli and Ganguly, 2016]. This in turn produces more dust activity in the form of both blowing dusty days and abrupt dust storms. According Lee and Gill (2015), excessive drought was identified as one of the main factors that influenced the emergence of Dust Bowl in 1930's. Drought contributed to the Dust Bowl by reducing soil cohesion, making it more erodible, and land cover, leaving the soil less protected from wind action. These same mechanisms operate today. Therefore, it is of crucial importance to understand the relationship between dust storms and drought intensity in order to model and predict dust storm scenarios including those which have an effect on highway safety. Given these factors, we explored the relationship between dust storm source points and drought intensity in the states of Texas, New Mexico, and Oklahoma as defined in the project plan.

The objectives of this study were three-folded: 1) to identify the spatial and temporal distribution patterns of hotspots that may contribute dust blowing to highways in the southwestern United States, 2) to identify the characteristics of the dust emission hotspots in relation to the distribution of highway, geomorphology, and land use, and 3) to classify the hotspots for the potential of blowing dust production based upon field observations and dust emission modeling.

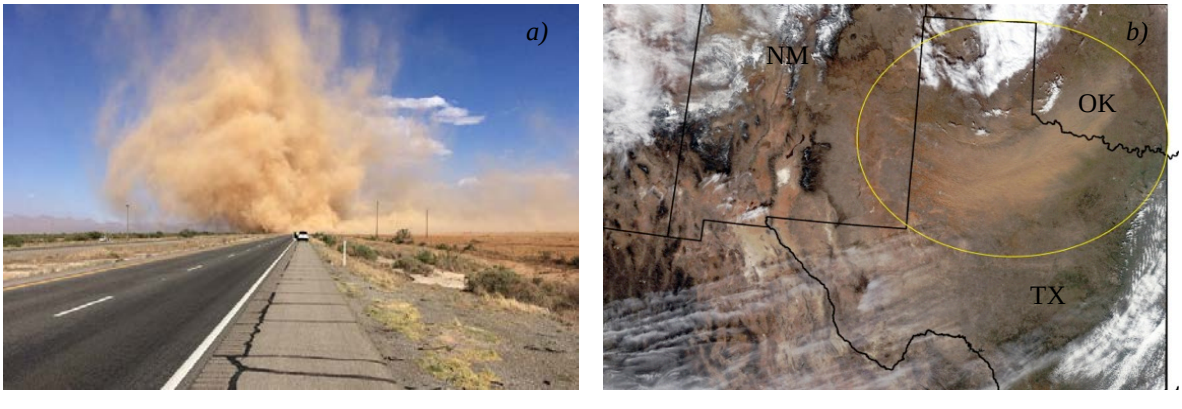

Figure 1. Illustration of dust events in the southwestern U.S. a) example of blowing dust passing across a highway in San Simon, southeastern Arizona, May 16, 2016 (Source: Arizona DPS), and b) example of dust plumes shown on NASA's Aqua MODIS true color imagery in northern Texas, January 22, 2012.

PART I. The spatial and temporal distribution of dust emission hotspots

1.1 Overview

Despite the widespread media attention of chain-reaction traffic incidents and property damage caused by windblown dust in the U.S. and elsewhere in the world, very few studies have investigated the relation of accident rates to windblown dust. Identification and cataloging of dust emission hotspots in a region allows for improved numerical modeling of the evolution of individual dust plumes and better forecasting of the onset and end of dust storm conditions, therefore representing a first step to manage and mitigate hazardous blowing dust's impact on highway safety. Various approaches, including frequency statistics, model simulation, and remote sensing, have been developed to identify dust emission sources (e.g., Ginoux et al., 2001; Prospero et al., 2002; Rivera Rivera et al., 2010; Park et al., 2010; Parajuli et al., 2014). These approaches, each with its own advantages and weaknesses, are largely constrained by the availability of the data (e.g., model input data, remote sensing imagery etc.) and the geographic scale of the research area.

1.2 Methods

1.2.1 Hotspots identification

Lee et al. (2009, 2012) developed a methodology to identify dust sources and their associated geomorphic and land cover characteristics in western Texas and New Mexico. In this method, meteorological records were used to determine the occurrence of airborne dust, and satellite images were used to identify dust sources. Days for image analysis were determined when the visibility drops to 5 km or less for at least 1 hour. The meteorological data were obtained from the U.S. National Weather Service at 15 representative cities within the study area. The dust sources were further identified using the true color MODIS (Moderate Resolution Imaging Spectroradiometer) imagery for the period of 2010 to 2016. The imagery has a pixel size of 250 m.

To further improve the dust source identification, a "split-window" technique was applied to enhance the dust in scenes, based upon the brightness temperature difference between the MODIS thermal channels of 31 and 32 (Baddock et al., 2009). The resulting image has dust plumes enhanced as black, while water, ice, and clouds show

up as white. It is noteworthy that dust events would not be apparent in the imagery if cloud cover obscured the ground or the timing of the satellite overpasses in relation to the dust occurrence. Additionally, convective dust events (initiated by downdrafts from thunderstorms) generally cannot be resolved in MODIS imagery. Dust plumes were identified in each image and the latitude and longitude of the upwind origin of each plume were identified using the procedure developed by Bullard et al. (2009) and Lee et al. (2009).

1.2.2 Relating the distribution of drought and dust emission hotspots

By creating a database of dust event locations and drought intensity and plotting them into GIS software (ArcGIS 10.3, ESRI, Redlands, CA), we performed a visual and statistical comparison between the drought intensity and dust storm source points. We viewed the drought intensity at dust storm source points on the nearest day to the dust occurrence, as well as the history of drought by calculating the average 1-year, 2-years, and 5-years drought accumulation at those points prior to the dust events. We considered also the spatial relationship between drought as defined by the Drought Monitor and dust points at different spatial coverages of single pixel, 30 km buffer distance, 60 km buffer distance, and 100 km buffer distance around the dust points.

The Drought Monitor data is produced and released weekly and classifies the drought intensity occurring at that time at any point in the USA into five major categories (http://droughtmonitor.unl.edu/) as well as a drought-free categorization. These five categories of drought types are: D4 (exceptional drought), D3 (extreme drought), D2 (severe drought), D1 (moderate drought), and D0 (abnormally dry). As an example, **Error! Reference source not found.** shows the U.S. Drought Monitor data for the contiguous U.S. for the week of September 1, 2009. For this study, the data from January 04 2000 to April 11 2017 and covering the whole U.S. were acquired, though only data for the states of Texas, New Mexico and Oklahoma, our Area of Interest (AOI) were used. The data are available in shapefiles of polygons which can be imported, managed, mapped, and analyzed in GIS software.

1.2.3 Data Processing

First the USDM associated with our AOI was extracted using the Intersect Tool (Analysis Toolset) in ArcToolbox. Because there are nearly 890 shapefiles in USDM, a script in Python was developed to accomplish the batch process of extraction through the Intersect tool. We also converted polygons to raster using the Polygon to Raster Tool (Conversion Toolset) in ArcToolbox. In this conversion, we used -110º to -93º longitude and +25º to +38º latitude as the coordinates of conversion extent and 0.1º x 0.1º as cell size of the raster output. The raster is saved in geotiff file format, so that the file can be easily imported to Matlab for further analysis.

1.3. Results

1.3.1 Spatial distribution of the hotspots

A total of 1625 dust storm source points, 827 from 2001 to 2009 and 798 from 2010 to 2014 were identified and their geographic locations were also determined (Figure 2, Table 1). Dust emission sources were located in U.S. and Mexico: only sites in the three U.S. states of interest were considered for this part of research (Figure 3). In this area, a total of 1187 dust emission hotpots were identified and located. Both figures 2 and 3 show that dust emission hotspots are highly concentrated in the southern Great Plains area in Texas. Some hotspots are also found in southeastern Colorado, southwestern Kansas, and southwestern New Mexico.

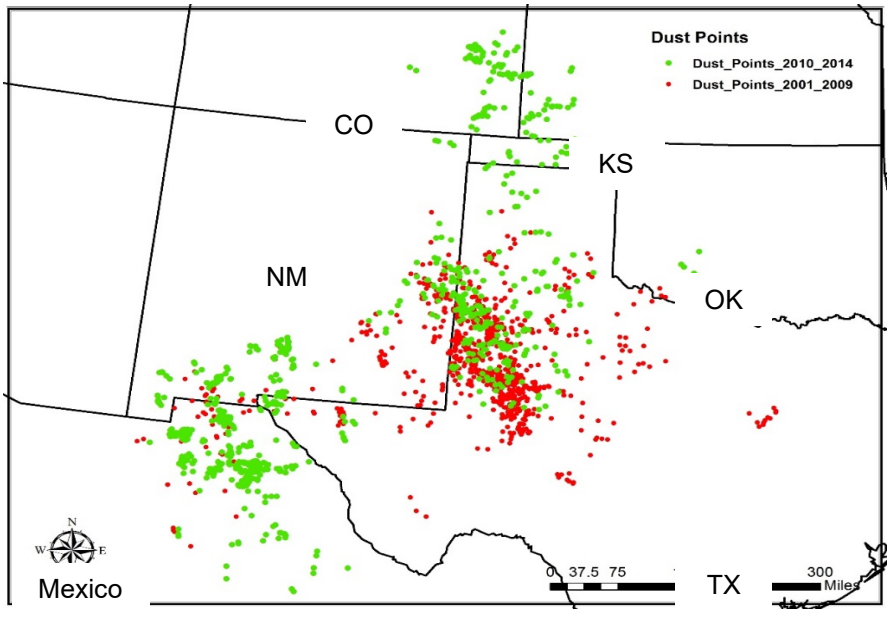

Figure 2. The distribution of dust emission hotspots in southwestern US and northern Mexico for the period of 2001 to 2014.

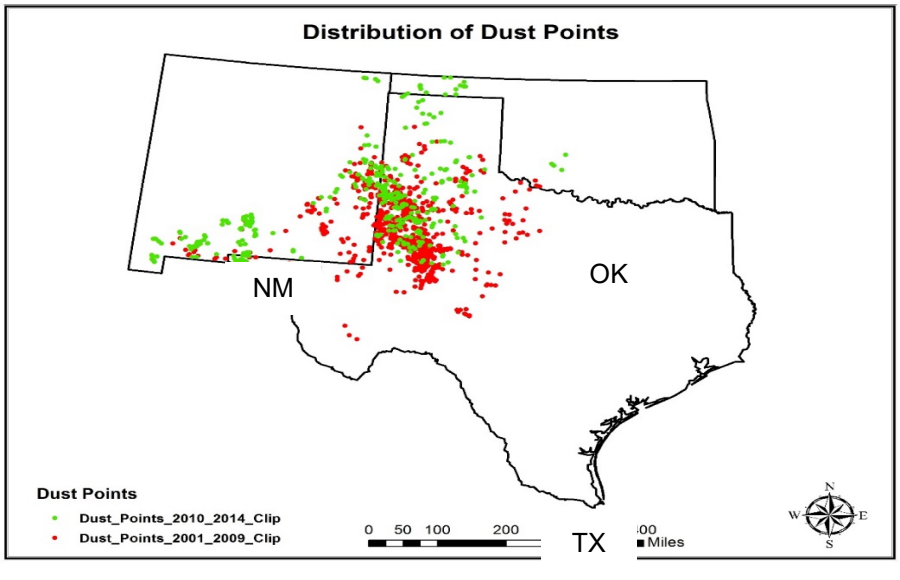

Figure 3. The distribution of dust emission hotspots in the area of interests (AOI), including the states of Texas, Oklahoma, and New Mexico.

1.3.2 Temporal distribution of the hotspots

For the case of Texas, the figures (Figure 4) show that during the time periods prior to the highest frequency distribution of dust storm events experienced excessive drought. For example, looking to the yearly frequency distribution of dust points, higher frequency is observed during 2003, 2008, and 2012. During the time frame before these years an excessive drought was also experienced. New Mexico (Figure 5) also shows the same evolution as that of Texas. In both states, it appears that intense droughts between 2001 - 2003, and 2011 - 2014 led to significant amounts of dust events in 2003 and 2012, respectively. In Oklahoma (Figure 6), the lowest frequency of dust events is observed and the events were mostly concentrated in 2005, 2012, and 2014. Prior to these observations there was an extreme drought between 2011 and 2012. The analysis of the combined data of the three states follows the same trend as that of the individual states (Figure 7). There was a significant drought generally over the three-state region in the time periods 2001 – 2006 and 2011 – 2015. In connection to these trends there was also a high number of dust events after these droughts.

Table 1. Number of dust emission hotspots identified in different regions in the study area.

Regions	TX	NM	OK	CO	KS	Mexico	Total
# Dust sources	888	278	21	72	30	336	1625

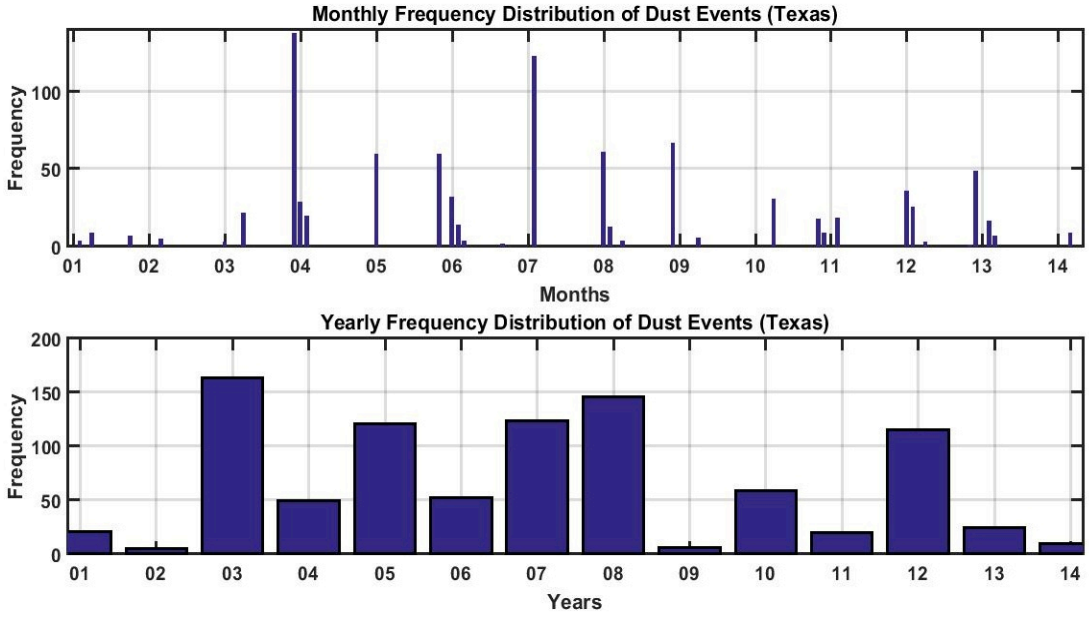

Figure 4. Monthly and yearly frequency distribution of dust storm source points for Texas.

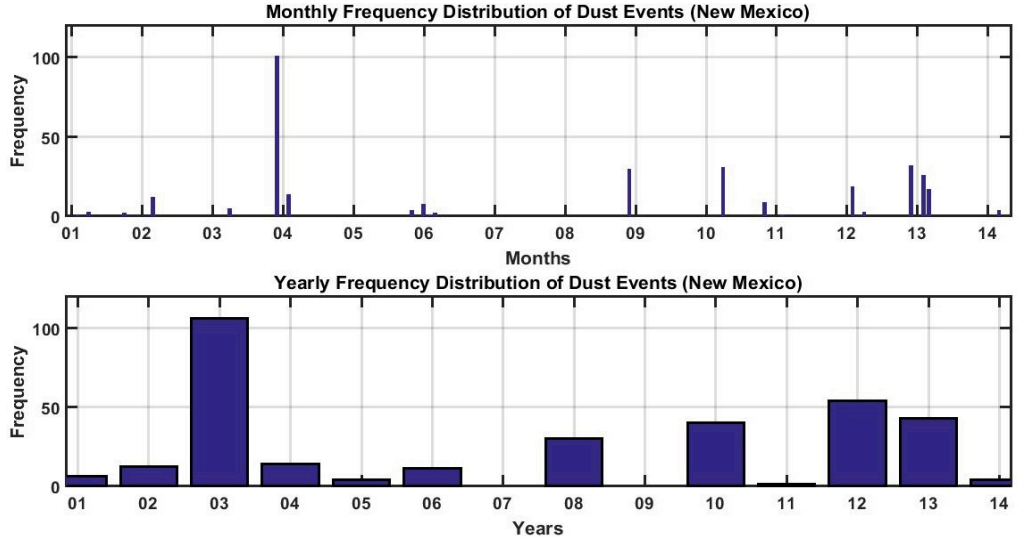

Figure 5. Monthly and yearly frequency distribution of dust storm source points for New Mexico.

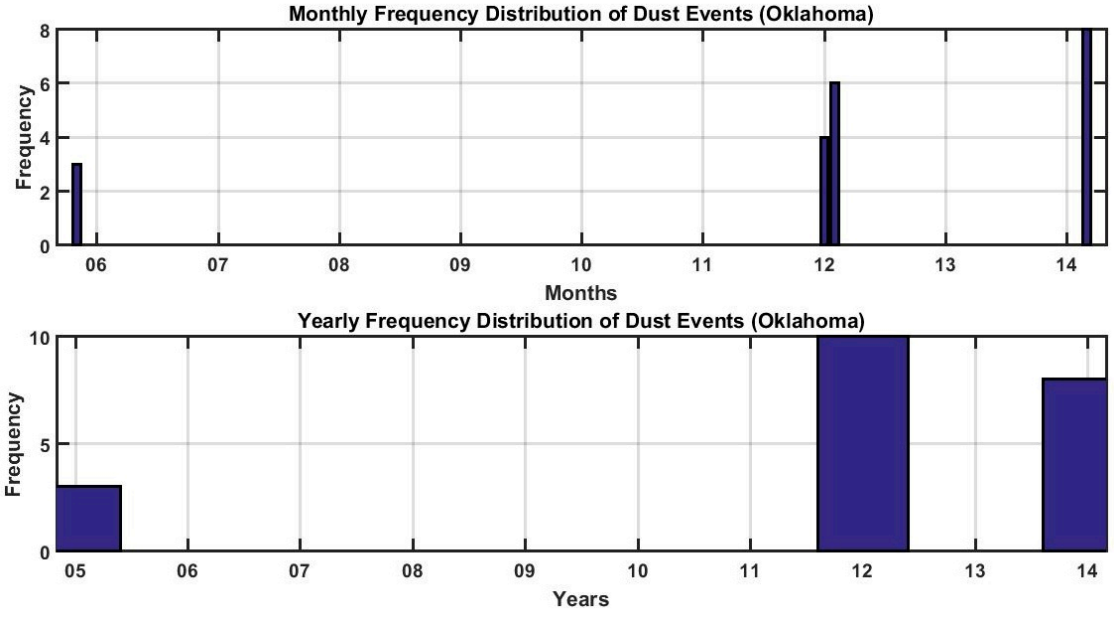

Figure 6. Monthly and yearly frequency distribution of dust storm source points for Oklahoma.

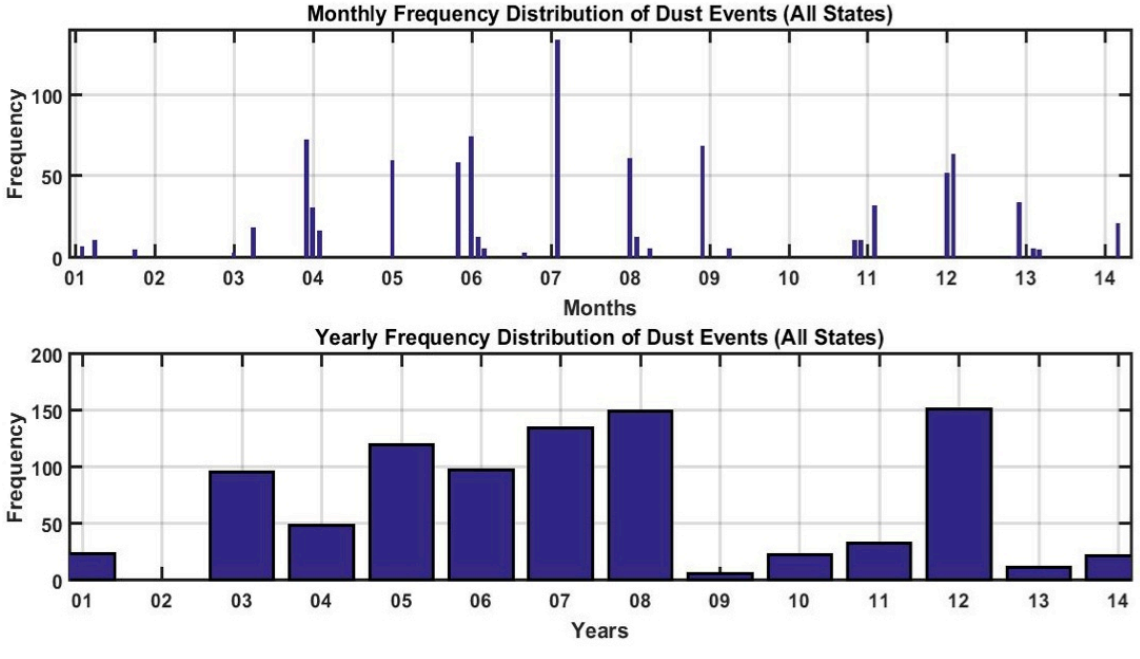

Figure 7. Monthly and yearly frequency distribution of dust storm source points for the three states (Texas, Oklahoma, and New Mexico).

1.3.3 Drought and hotspot distribution

The overall mean map shows the highest average value of drought intensity in the Southern part of Texas and extending between Southwestern part of Oklahoma and Northeastern part of Texas (Figure 8). The lowest overall average drought intensity is experienced in the Eastern part of our study region and large part of New Mexico. Most of the study area displays an intermediate strength of drought intensity. The total sum map of drought intensity shows almost the same spatial distribution of drought intensity as of the overall mean map, their only difference is that New Mexico experienced a high value of total sum drought intensity.

Figures 9 and 10 show that the dust points with highest drought intensities are concentrated on the Southern High Plains region, more specifically in a belt extending from the west to the south of Lubbock, Texas. This is a region where land use is predominantly dryland cropping- i.e., active growing of plant crops relying on natural rain, without irrigation. In such a land use, periods of drought would necessarily be associated with crop failure and reduced land cover, which would increase the wind erodibility of the land surface. We can infer from this observation that the excessive drought in combination to the use of the land for dryland agriculture in this region may contribute to most the significant number of dust events. The other two maps also bolster the aforementioned observation, with the total sum and overall mean of drought intensity also highest in the dryland agriculture region around Lubbock, especially to its south and west.

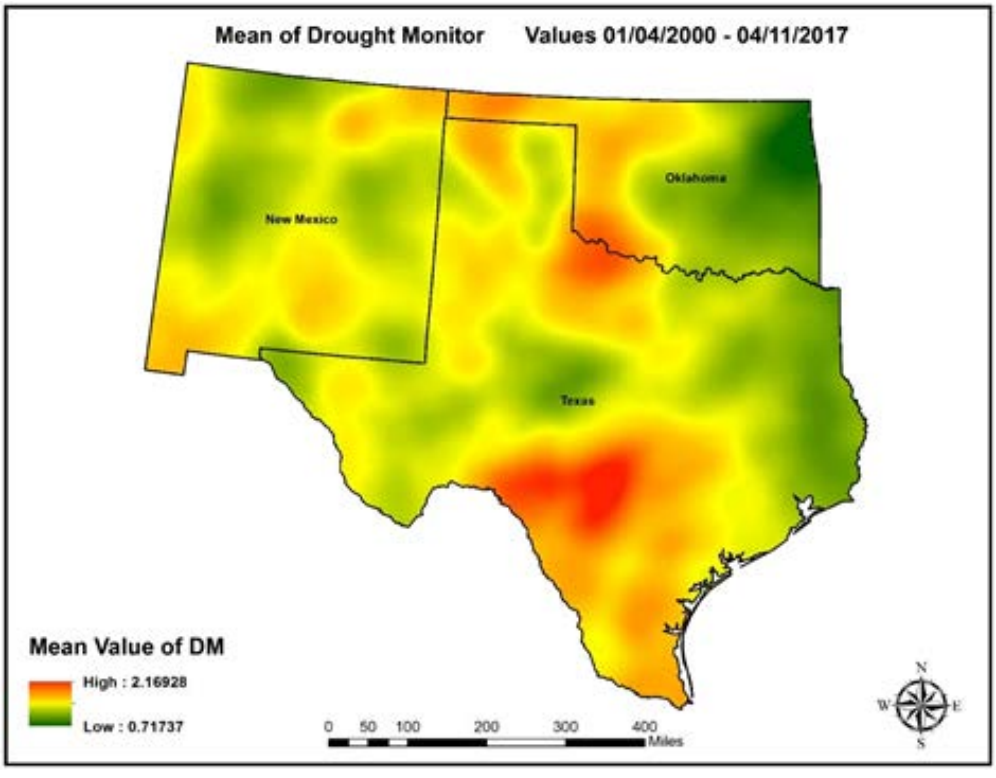

Figure 8. Overall mean of USDM values (Jan. 4, 2000-Apr.11, 2017).

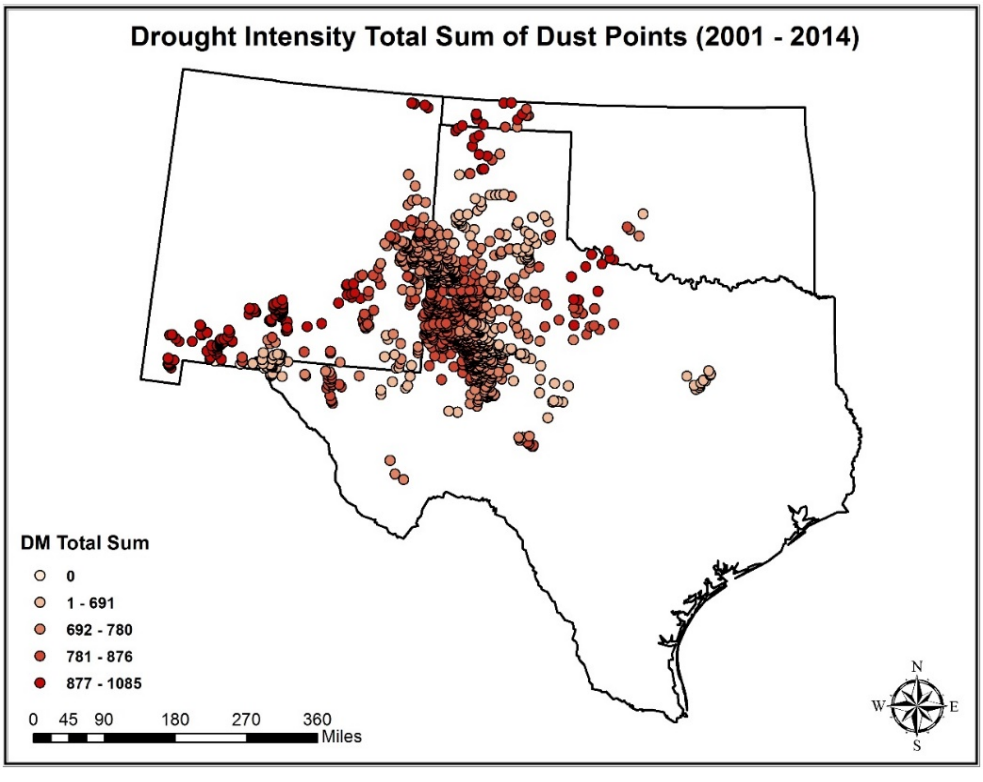

Figure 9. Drought intensity at the time of each dust event (2001- 2014).

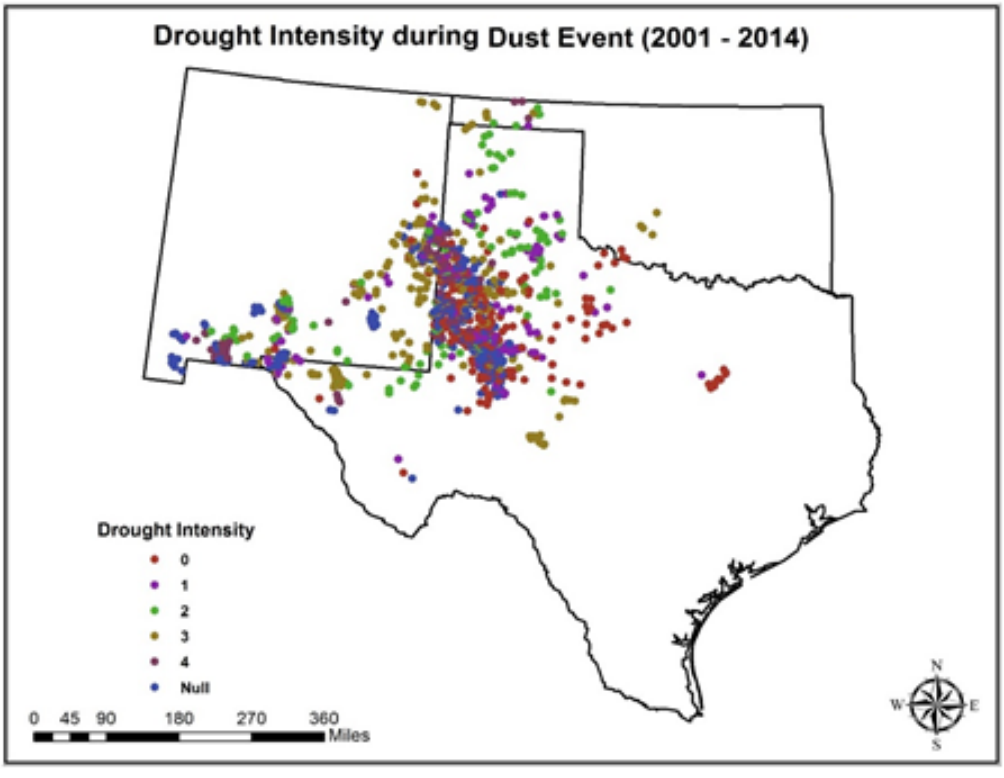

Figure 10. Sum total of drought intensity at each dust point (2001- 2014).

PART II Characteristics of highways, land use, and geomorphology at dust emission hotspots

2.1 Overview

In PART I, the distribution of the dust emission hotspots and their geographic locations were determined. In this part of the study, we investigated the characteristics of highway, land use, and geomorphology with the associated dust emission hotspots. The study area was defined using United States Department of Agriculture Major Land Resource Areas (Austin, 1965) for the Southern High Plains and extending westward into known dust-producing regions in the Chihuahuan Desert of New Mexico, and northward into north Texas and the intersection areas of Texas, Oklahoma, Kansas, and Colorado. In addition, we focused on the time period of 2010-2016, as we used the 2011 land use data to derive the land use and geomorphologic features.

2.2 Methodology

Land cover map was obtained from the National Land Cover Dataset produced by the Multi-Resolution Land Characteristics Consortium (MRLC). The latest database of NLCD 2011 was used. These land cover data are available at 30 m resolution and were derived primarily from Landsat images. We generally followed Level II of the U.S. Geological Survey land use and land cover classification system. The land cover map was overlaid with both the observed point sources and the highway distribution map to allow the determination of number of dust sources from each land cover type and their relative locations to the adjacent highways. For the purpose of this study, we focused on the interstate highways, U.S. numbered highways, and those highways with speed limit > 80 km/hour (equivalent to 50 mph in the U.S. highway system).

The Bullard et al. (2009; 2011) dust emission geomorphology classification system was applied to a base map of landscape unit polygons in order to create the geomorphology map. We used a 1:250,000 scale soil units map obtained from the Digital General Soil Map of the United States or STATSGO2. According to Lee et al. (2012), there is a close relationship between soils and geomorphology in our study region. A total of 17 geomorphic categories were identified based on the interpretation of surface geology and soil maps, and soil polygons were then attributed to one of these geomorphic categories.

We then overlaid the observed dust emission point sources on the two maps to determine the number of dust sources for each geomorphic or land use category. We further calculated the “dust emission” ratio, which is calculated by dividing the percent of total dust source points in each geomorphic or land cover category by the percent of total area occupied by the category (Lee et al., 2012). The dust emission ratio allowed us to describe the relative dust production of a category of land use or geomorphic feature.

For the distribution of the roads, we focused on the interstate and principal highways with speed limit >50 mph. We conducted a proximity analysis in ArcGIS (ArcGIS 10.3, ESRI, Redlands, CA) to determine the distance of hotspots to the neighboring

highways. The hotspots located within 1 km to adjacent highways were subject to further analysis described in the following sections.

2.2.1 Field verification, measurements, and laboratory analysis

A field campaign was conducted in June 2016 with the purpose to verify dust source remote sensing analysis, and to measure threshold shear velocity (TSV) of wind erosion on dust emission hotspots. TSV depicts the erodibility of soil surface and it is a key parameter in wind erosion observation and quantification. TSVs were estimated using a method developed by Li et al. (2010). In this method, TSV was quantitatively related with the resistance of the soil surface to disturbances created by a penetrometer and projectile shot by an air gun at the soil. At each hotspot location, 10-15 repeated air gun and penetrometer measurements were conducted along three 50-m transects oriented at 100°, 220°, and 340° from due north. At the time of TSV measurement, the volumetric soil water content was also measured using a hand-held time-domain reflectometer (TDR 100, Spectrum Technologies Inc., Aurora, IL) with 12 cm probe rods. Finally, for shrubland and grassland hotspot sites, height and width of plant canopies along the transects were also recorded.

In the verification exercise, a total of 55 hotspots, located within 1 km to adjacent highways, were located and assessed with regard to land use/land cover, crop grown, irrigation, and surface conditions (e.g., crust, crop stems etc.). These hotspot sites were accessible via non-private roads.

Finally, at each hotspot site, a composite soil sample was collected from the top 5-cm soil profile. Soil samples were processed and analyzed for texture and particle-size distribution using a laser diffraction Malvern Mastersizer 2000 particle-size analysis system (Malvern Instruments, Worcestershire, UK). For this analysis, we followed the protocols of Sperazza et al. (2004) and dispersed a subsample of approximately 0.9 g (obtained using a box splitter) in sodium hexametaphosphate solution and measured for grain size. Organic matter was not removed from the subsamples before the grain size analysis.

2.3 Results

2.3.1 Distribution of the hotspots

For the period of 2010-2016, a total of 620 dust emission hotspots were identified and located. Dust events associated with these hotspots are highly seasonal (Figures 11, 12). More than 50% of the dust events occurred from February to March and nearly 40% occurred from November to December. No dust events were identified from May to October during our study period. Annually, the year of 2012 had notably higher number of dust events than the rest of the years. Data for 2015 was not available as we were not able to obtain cloud-free MODIS images for the study area at the times of dust events.

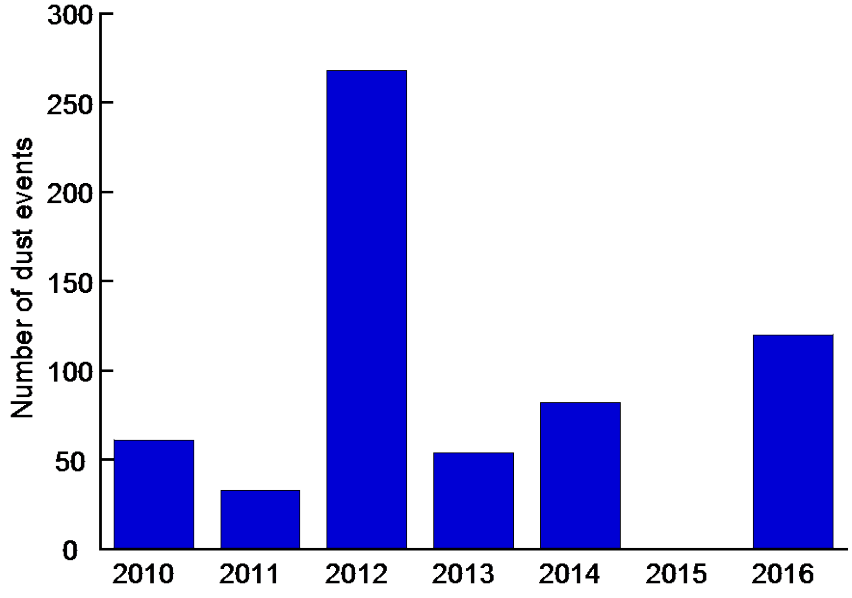

Figure 11. The annual distribution of the dust events that were associated with dust emission hotspots identified during the period of 2010-2016 in the study area. Note the 2015 data was missing because no cloud-free MODIS images were obtained.

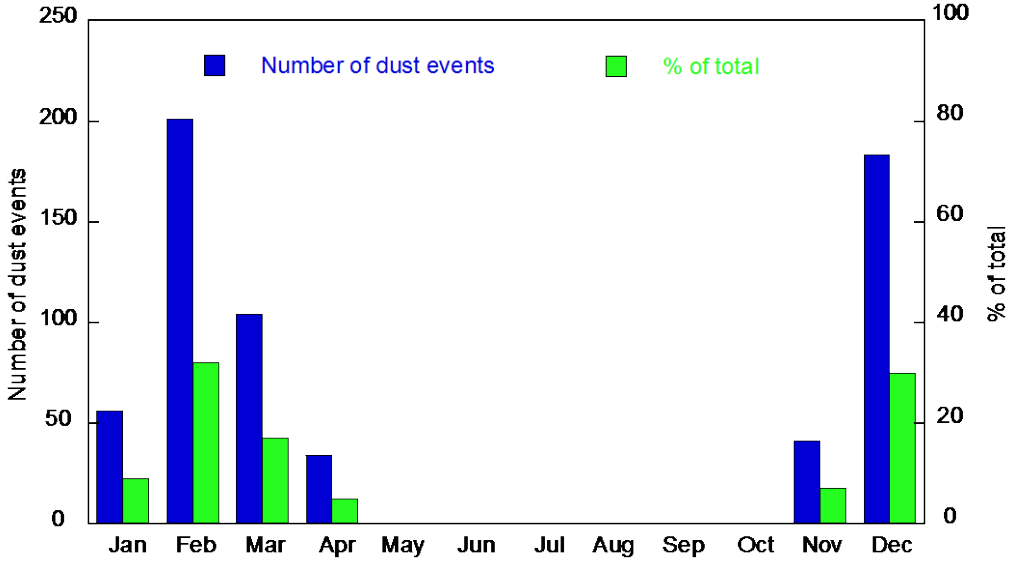

Figure 12. The monthly distribution of the dust events that were associated with dust emission hotspots identified during the period of 2010-2016 in the study area.

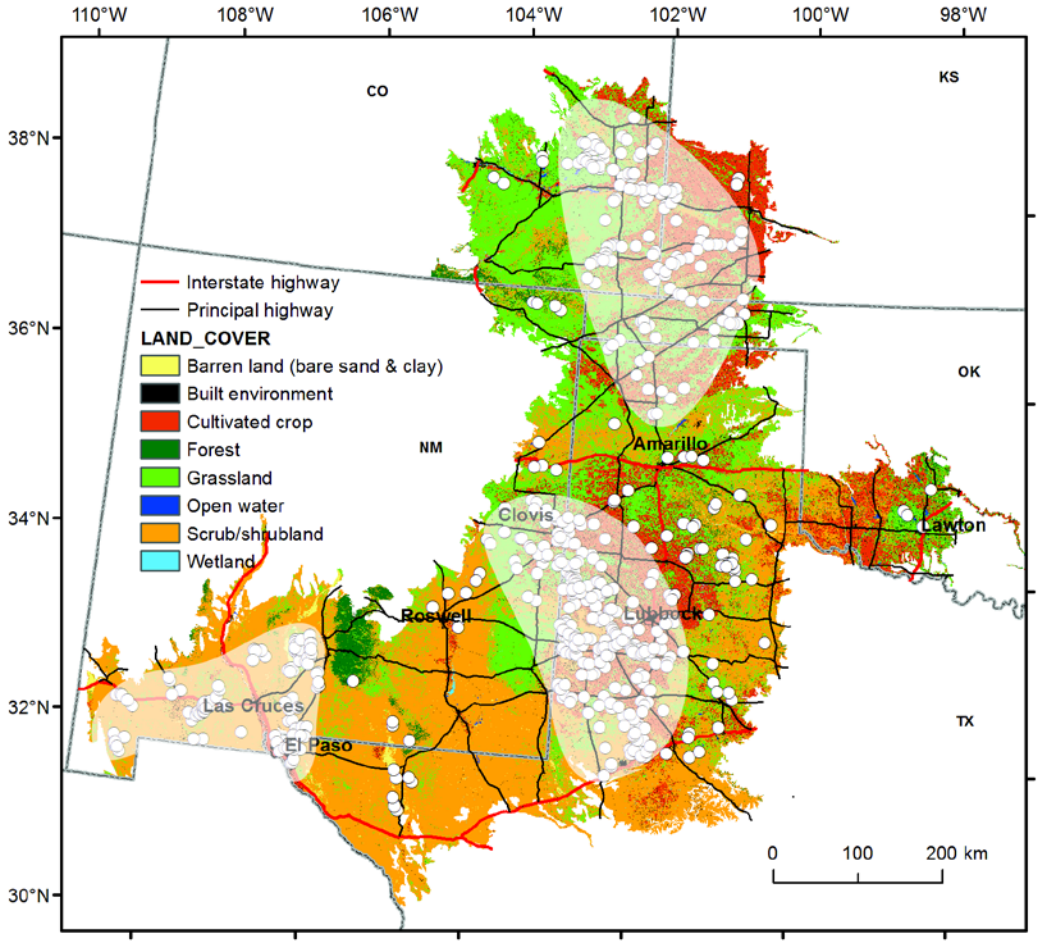

Figure 13. The spatial distribution of the dust emission hotspots (white circles) and the associated land use on the surface, and their relative locations to the highways in the study area. The shaded areas are the approximate distribution of the three primary dust emission hotspot regions.

The spatial distribution of the hotspots and their associated types of land use in the study area are shown in Figure 13 and Table 2. In the study area, the primary land use classes include cultivated crop (21%, hereafter called cropland), shrubland (41%), and grassland (31%). Of the 620 total hotspots, 234 (38%), 164 (27%), and 141 (23%) are located on cropland, shrubland, and grassland, respectively. These hotspots are generally centralized in three primary regions: north region (north of Interstate Highway I-40), south-central region (centralized in the Lubbock, Texas and Clovis, New Mexico area, including part of the Interstate Highways I-40 and I-27), and the Chihuahuan Desert region (centralized in the El Paso-Las Cruces-Deming area with the primary Interstate Highways of I-10 and I-25). In the north region, most of the dust sources occurred on grassland and cropland, whereas in south-central region, a majority of the dust sources were located on the cropland. Finally in the Chihuahuan Desert region, nearly all dust sources were found on shrubland.

The buffering analysis showed that of the 620 total dust emission hotspots, 75 (or 12%) are located less than 1 km to adjacent highways, and these hotspots are located primarily in the south-central region (Figures 14, 16). Among these hotspots, 8 are

located close to interstate highways (e.g., I-10), and 67 are located close to local highways. In terms of land use, 34, 25, and 4 hotspots are located on cropland, shrubland, and grassland, respectively (Appendix 1). Figure 15 also shows that more than 70% of the hotspots are located within 10 km of a nearby highway in our study area.

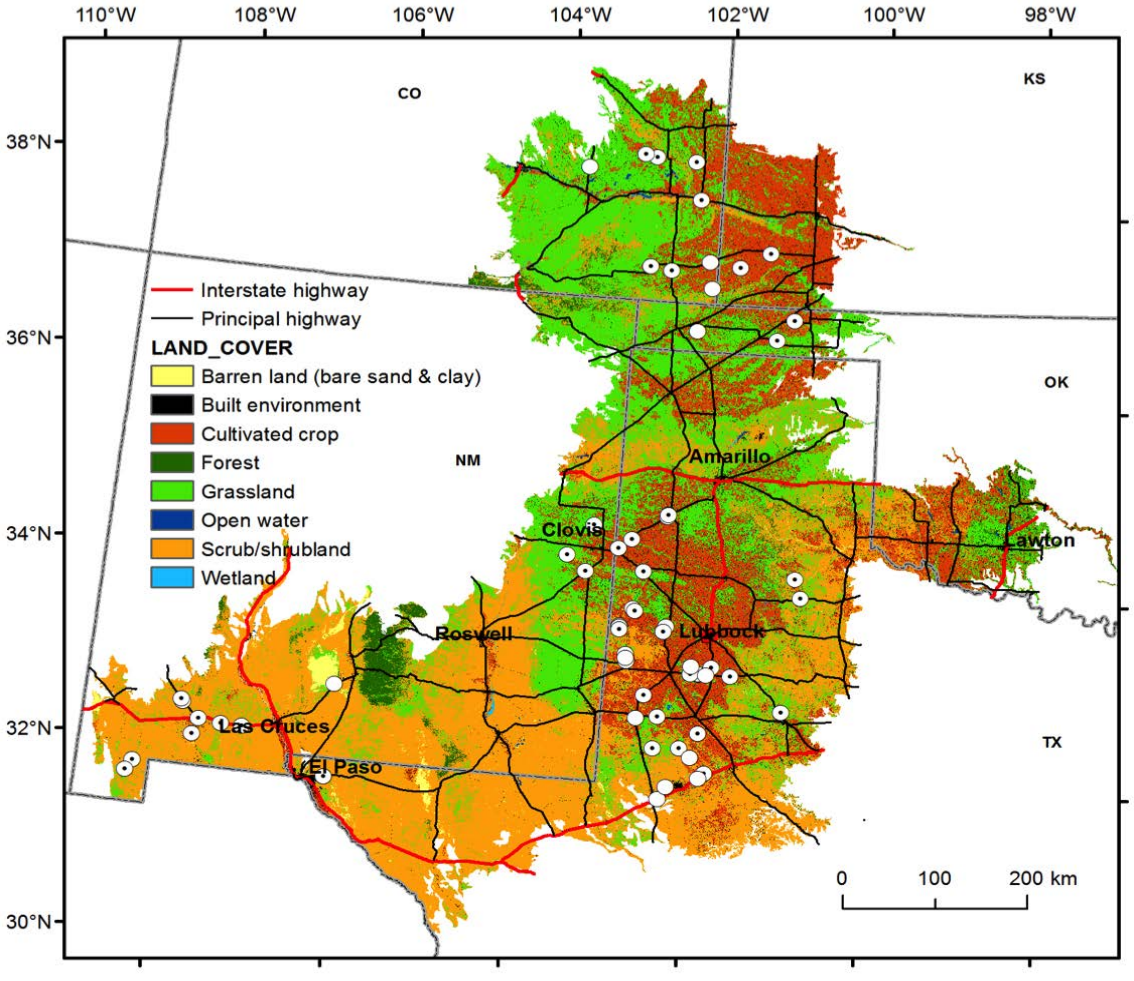

Figure 14. The spatial distribution of dust emission hotspots that are located within 1 km to the adjacent highways. White dotted circles denote the 55 hotspot sites where field verification and investigation were conducted. These are also the sites where the blowing dust emission potential was evaluated by WEPS modeling

The spatial distribution of the hotspots and their associated geomorphic surfaces are shown in Figure 15 and Table 3. Similar to the land use map, these sources are concentrated on two primary geomorphic surfaces, sand sheet and alluvial, which account for 48% and 25% of the total dust sources in the study area. It is noteworthy that ephemeral lakes, only account for 1% of the total surface area, however account for 8% of the total dust emission sources.

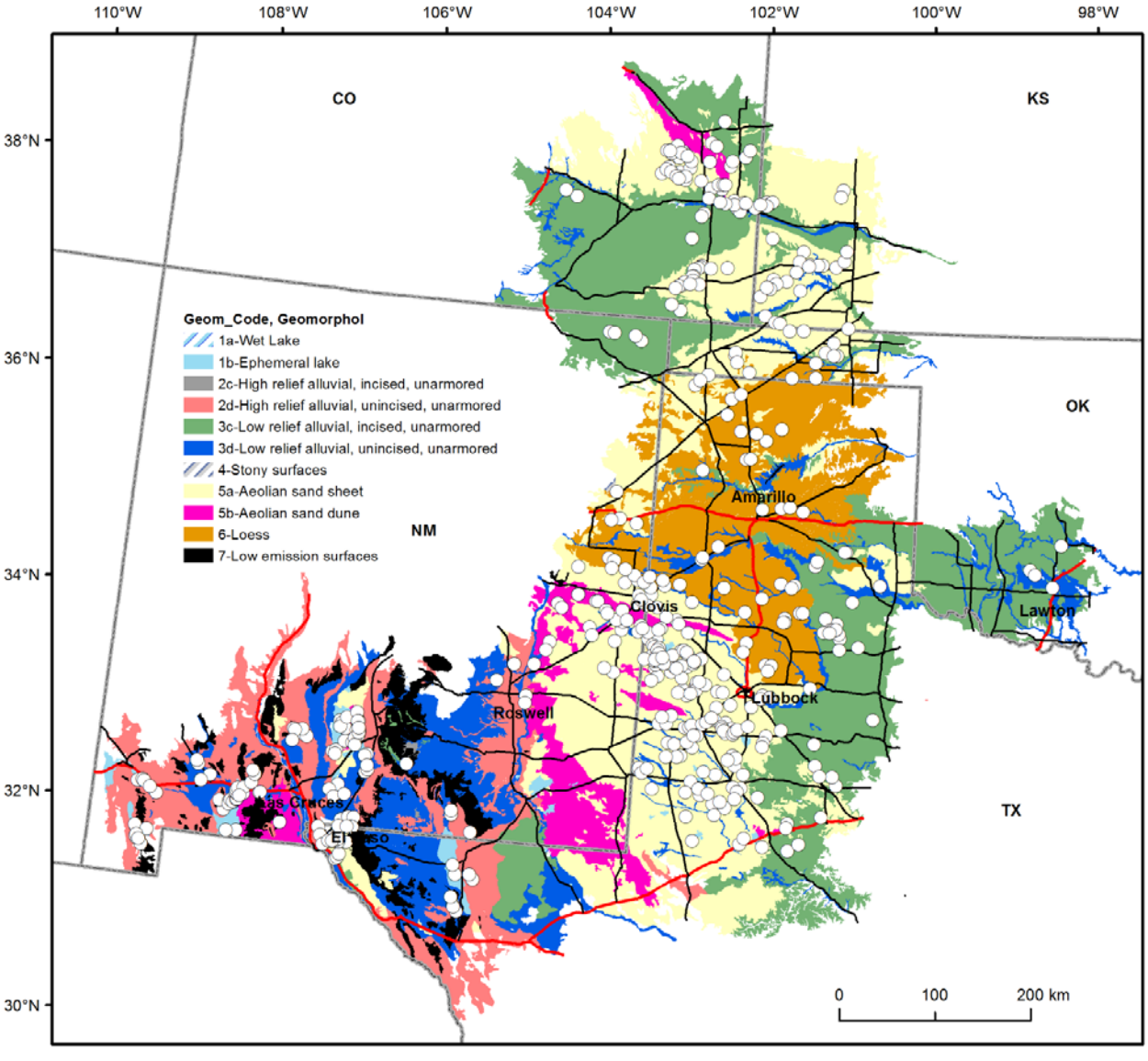

Figure 15. The spatial distribution of the dust emission hotpots and the associated geomorphic features in the study area.

Table 2. The distribution of the dust emission hotspots in relation to land use in the study area.

Land use	Grassland	Cropland	Barren land	Shrubland	Forest	Urban
Area (%)	31	21	1.2	41	4	1
Dust source point (%)	26	36	6	27	2	1.5

Table 3. The distribution of the dust emission hotspots in relation to geomorphology in the study area.

Geomorphology	Alluvial	Loess	Sand sheet	Ephemeral lake	Dunes	Other
Area (%)	48	12	29	1	6	4
Dust source point (%)	25	8	48	8	8	3

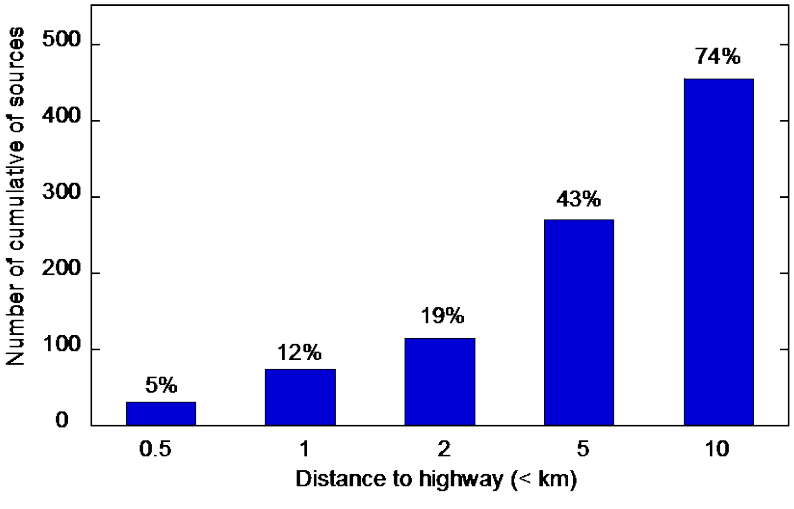

Figure 16. Distribution of the dust emission hotspots relative to adjacent highways. Numbers on top of each bar indicate the cumulative percent of hotspots as the distance increase from 5% for a distance of 0.5 km to 74% for a distance of 10 km away from the adjacent highways.

The dust emission ratios further show that barren sand has the highest emission ratio among all types of land use, whereas ephemeral lake has the highest emission ratio among all geomorphic surfaces (Figures 17, 18). The lowest emission ratio was found on forest (land use) and alluvial surface (geomorphology).

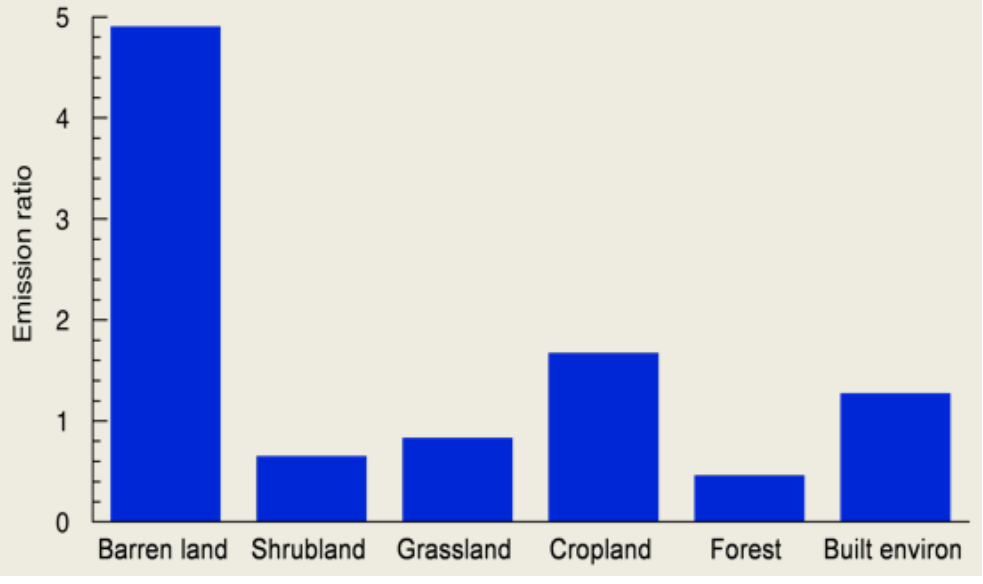

Figure 17. Dust emission ratios for different types land use in the study area.

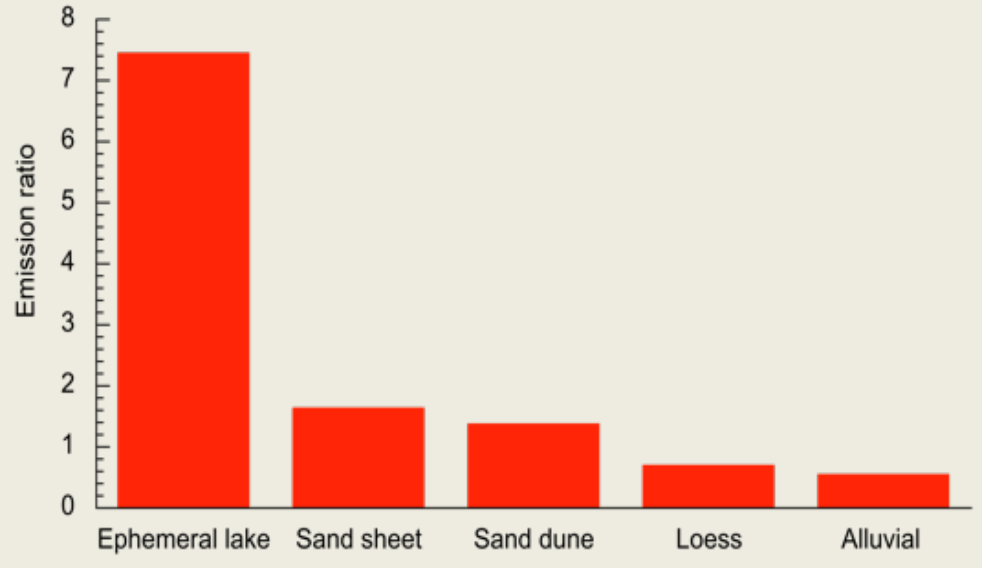

Figure 18. Dust emission ratios for different types geomorphic surfaces in the study area.

2.3.2 Dust emission potentials from the hotspots

Soils at the hotspot sites that are located within 1 km to adjacent highways are dominated by sand and silt particles, despite the fact that they are located on different types of land use (Figure 19, Appendix 1). Except for the hotspot sites that are located on barren sandy land, soils at the hotspots generally have abundant supply of fine particles, e.g., particles with diameter of 50-100 μm, giving them a greater potential of generating dust plumes from wind erosion.

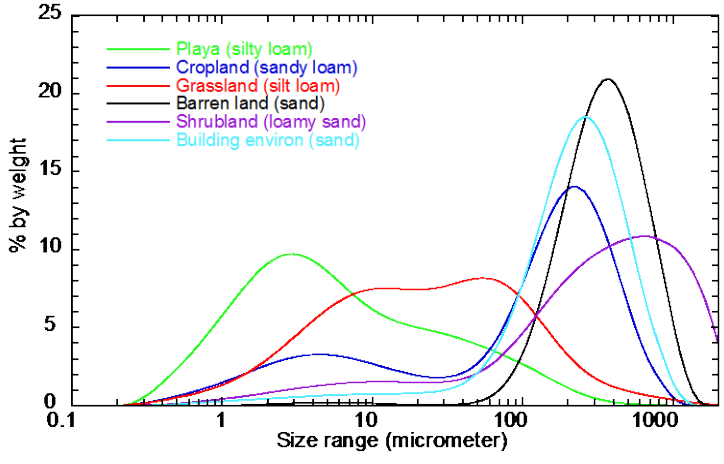

Figure 19. Particle-size distribution of soils from representative dust emission hotspots located at different land uses identified in this study. For playa and grassland soils, particles with size <100 μm are dominant, but the percent of coarser particles increased substantially for soils located on cropland, shrubland, barren land, and building environment. Dotted area indicates range of soil particle size (50-100 μm) which is generally found to have lower threshold shear velocity and therefore is more susceptible to dust emission (Marticorena and Bergametti, 1995).

Threshold shear velocities (TSVs) for the surface soil at individual hotspot sites and different types of land use in the study area are show in Figure 20 and Appendix 1. These results show that TSVs on the different types of land use are not significantly different, except for the barren land, which has significantly lower TSVs than those of the other types of land use. Figure 21 also shows that disturbed soils could have much higher potential to produce blowing dust than that of the undisturbed soils (e.g., surface protected by physical or biological soil crust), illustrated by significantly higher TSVs. For example, average TSVs for undisturbed and disturbed playa sites are 1.15 m s^{-1} and 0.35 m s^{-1}, respectively. At the time of TSV measurement, soil water content at the hotspot sites was moderate and varied from 5% to 20% (data not shown).

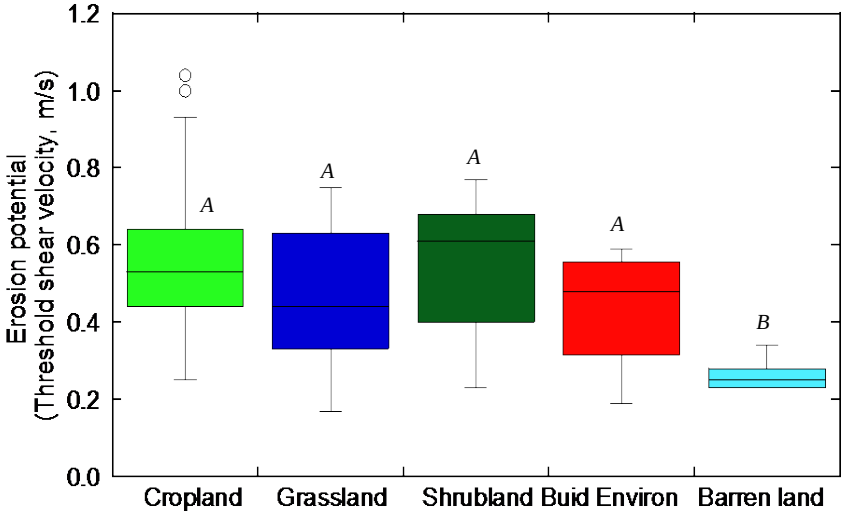

Figure 20. Box plots showing the characteristics of threshold shear velocity (TSV) of surface soil measured from primary land use in the study area. *a*) Box plot of TSV, *b*) TSV for disturbed and undisturbed surfaces. Different letters indicate significant difference (p<0.05) between different land uses by ANOVA.

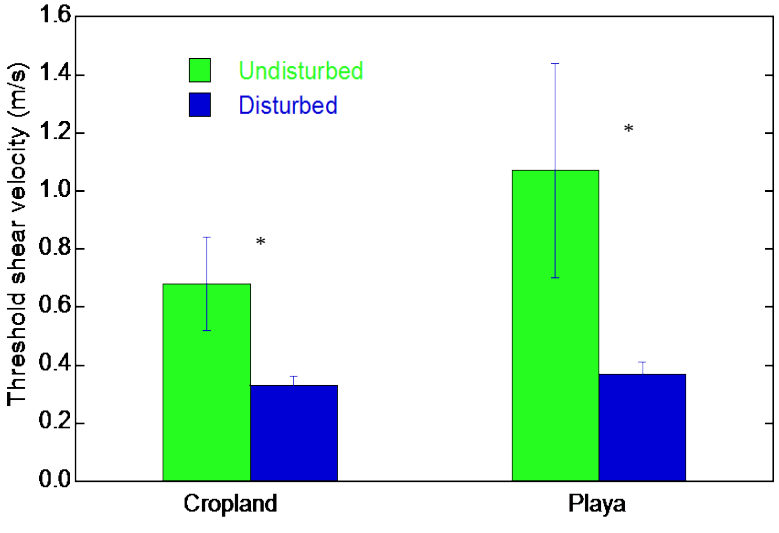

Figure 21. Characteristics of threshold shear velocity (TSV) of surface soil measured for disturbed and undisturbed surfaces. * indicatse significant difference (p<0.05) between different land uses(*t*-test).

PART III Simulation of blowing dust from dust emission hotspots

3.1 Overview

While the previous sections answered the questions where the dust emission hotspots are located their characteristics of land use and geomorphic surfaces, the questions of when and how much dust may be produced from these hotspots are still not answered. In this part of the study, we used an up-to-date wind erosion model to estimate dust emission from the individual hotspots, and to identify the time periods when the risk of hazardous blowing dust may be produced.

For this part of the study, we only focused on the 55 hotspots where are located within 1 km to adjacent highways. Also, these are the dust emission sources that were validated and the necessary soil and vegetation properties for the modeling were also measured during a field campaign conducted in June 2016.

3.2 Methods

Dust emissions from the hotspot sites were estimated using an up-to-date Wind Erosion Prediction System (WEPS, v.1.5.52, released Nov 30, 2016). WEPS is a physical process-based daily time-step computer model that simulates weather, field surface conditions, and erosion (Wagner, 2013). WEPS was developed in the Great Plains environment of the U.S. and the model has been extensively validated in similar settings and elsewhere in the world (e.g. Hagen, 2004; Feng and Sharratt, 2007; Buschiazzo and Zobeck, 2008; Feng and Sharratt, 2009; Li et al., 2014).

The principal datasets that are required to run WEPS include soil properties, climate and wind, and crop management data. The physical dimensions (i.e., shape, area, length, and width) and the orientation of the hotspot sites were determined by using Google Earth™ images. No patterned barriers were observed at any of the hotspots. Climate and wind input files were generated within WEPS and reflect historical weather records. WEPS simulations were conducted using the cycle mode with a simulation cycle of 50 years for each year in the crop rotation (e.g., a two-year wheat-fallow rotation would have a simulation of 100 years). A minimum of 50 years per rotation year is needed to fully reflect historical weather distributions.

The distribution of crops and their rotations were determined using the USDA-NASS Cropland Data Layer (CDL). The CDL is a raster, geo-referenced, land-cover dataset with a ground resolution of 30 m (NASS, 2015). The crop management files were obtained from the NRCS nationwide list of crop management zone files, which were developed by the NRCS based on typical crops and management practices employed on farms within each zone (Nelson et al., 2015).

Similar to geomorphic maps, the soil data was acquired from the USDA-NRCS Soil Survey Geographic (SSURGO) database and was downloaded via Simple Object Access Protocol (SOAP) from the NRCS Soil Data Mart website (NRCS, 2015).

WEPS simulations were conducted for all 55 hotspot sites that are located within 1 km to adjacent highways. Since suspension-size particles are the primary component of blowing dust, we reported flux of suspension particles and the time periods when the highest value of suspension was predicted by the WEPS model. WEPS considers particles <100 μm as suspension size.

It should be noted that WEPS was developed to simulate wind erosion on cropland, and appropriate adjustments must be made to the model's plant growth parameters and Management file in order to apply WEPS on non-cropland systems. For grasslands, we adjusted the generic "pasture" plant populations to represent those lands. For shrublands, we simulated a sparse perennial crop with parameters adjusted to grow similar plant geometry (i.e., canopy height, canopy width, fractional cover, leaf area index etc.) as found on shrublands in the study area, with the assumption that the shrubs are relatively uniformly distributed. For sites on both land uses, we also excluded tillage, harvest, irrigation etc., as they are not typically performed on grasslands and shrublands.

3.2.1 Classification of dust emission hotspots

For hotspots that are close to the highways, the amount of airborne dust, M, that is generated from an area of A during a wind event with duration of T, may be estimated as:

$$M = F \times T \times A \quad (1)$$

where F is dust emission (also called vertical dust flux) that represents the rate of particles that leave the surface area. F has a unit of mass per unit area per time and was estimated using the WEPS model for individual hotspot sites.

For a short period of time after the dust entrainment, the concentration of dust in the air (C_d, g m^{-3}) may be calculated as:

$$C_d = \frac{M}{A' \times H} \quad (2)$$

where A' is the area of the dust plume when it travels to the highway, and H is the height of the dust plume. For dust plumes that are relatively close to the source areas, we assumed $A'=A$, and H=100 m for a typical blowing dust event with strong winds.

Finally, visibility, V (m), is related to the concentration of dust in the air according to an equation developed by Patterson and Gillette (1977):

$$V^{\gamma} = \frac{C}{C_d} \quad (3)$$

where C and γ are empirical constants. For western Texas, Patterson and Gillette (1977) reported that the best values were C=2.0 × 10^{-2} g m^{-3} km and γ =1.07, when visibility measurements were made close to the dust source (e.g., <10 km). Using this method in combination with other field observations (e.g., Hagen and Skidmore, 1977; Baddock et al., 2014), we developed a visibility classification system related to

concentrations of dust in the air (Perry and Symons, 2002) (Table 4). The visibility and associated dust in the air were used to classify the hotspots based upon their hazardous dust production potential simulated by the WEPS.

Table 4. A visibility classification system that was used to classify the levels of hazard of dust emission hotspots to highway traffic.

Visibility	Concentration of dust in the air (mg m^{-3})	Levels of hazard to highway traffic	Comparable to foggy conditions*
< 200 m	> 110	I, Very High	Dense-Thick fog
200 m- 1 km	20-110	II, High	Fog-Thick fog
1 km-2 km	5-20	III, Moderate	Mist, haze
2 km -5 km	1-5	IV, Low	Poor visibility
> 5 km	< 1	V, Not Affected	Good visibility

* According to Perry and Symons (2002)

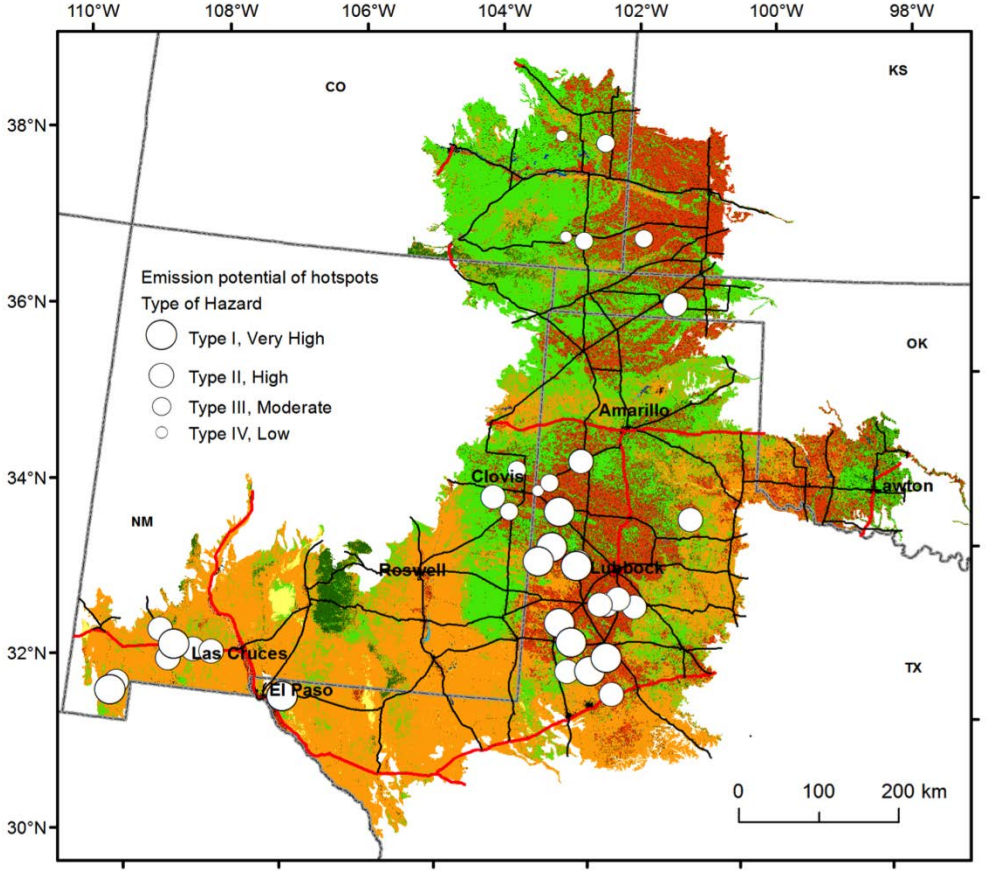

Figure. 22. Distribution of dust emission hotspots with different types of potential to produce hazardous blowing dust to highway traffic. Types of hazardous blowing dust are defined in Table 1 and the magnitudes of WEPS simulated suspension at the hotspot sites are listed in Appendix 1. Type V (Not Affected) dust emission sites were not shown in this map.

3.3 Results

WEPS simulations show that among the 55 hotspot sites that are located within 1 km to adjacent highways, 13 have the potential to produce annual dust emissions of >3.79 kg m^{-2}. These hotspots fall in the Type I (Very High) hazard to the highway traffic in the study area (Figure 22, Appendix 1). For these Type I hotpots, 8 are located in the south-central region with associated land use of cropland and 2 are found in the Chihuahuan Desert region on shrubland. The simulation results further revealed that the highest likelihood that these hotspots will produce hazardous blowing dust is in February and March (Appendix 1).

Up to 21 hotspots were classified to Type II (High) hazard to highway traffic, with estimated annual dust emission of 4.81-0.76 kg m^{-2}. Among these hotspots, 14 are located in the south-central region and 6 are located in the Chihuahuan Desert region (Figure 22, Appendix 1). The reminder of the 55 hotspots that are close to the highways were classified to have Type III (Moderate) to Type V (Not Affected) hazard to highway traffic, including a few hotspots that occurred on grassland and cropland in the north region of the study area.

DISCUSSION

In this study, we focused on the dust emissions from individual locations, i.e., hotspots, and their potential hazard to ground transport. We visually identified sources of dust emission on satellite images, aided by meteorological records and proven quality improvement techniques. This method, however, has some known limitations (Lee et al., 2009, Rivera Rivera et al., 2010; Lee et al., 2012). Most notably, because dust obscures the ground, dust sources beneath the dust cloud (i.e., downwind of the source) may not be detected, whereas upwind sources may be preferentially identified by this approach. In the case of this study, most dust events were associated with westerly or southwesterly wind (the prevailing wind direction in the study area, Lee et al., 1994; Novalan et al., 2007), so western, upwind sources were more likely to be identified. Additionally, precise location of source points is somewhat subjective because dust in ‘true color’ scenes is similar to the underlying ground surface. Lee et al. (2009) also pointed out that because erosion may occur before there is sufficient downwind plume development to make the plume observable in the image, the exact source points of some plumes may have been located a small distance upwind of where the 250 m MODIS pixel first indicated the presence of dust. Finally, as Baddock et al. (2009) pointed out, some dust activity is likely missed due to the relative timing of overpass and dust emissions as the satellites that MODIS aboard only pass twice per day. Despite the fact that the overall method for identifying the point sources for the event is less than perfect, it is arguably the best method available for the purpose of our study (Baddock et al., 2009). The temporal pattern of dust emission hotspots identified by this study is well in line with long-term field observations for two primary cities in the study area, i.e., Lubbock, Texas (Lee et al., 1994), and El Paso, Texas (Novlan et al., 2007).

The analysis of the relative distribution between dust emission sources the intensity of drought revealed that there was a significant drought generally over the three-state region in the time periods 2001 – 2006 and 2011 – 2015. In connection to these trends there was also a high number of dust events after these droughts. Additionally, dust points with highest drought intensities are concentrated on the Southern High Plains region, more specifically in a belt extending from the west to the south of Lubbock, Texas. This is a region where land use is predominantly dryland cropping- i.e., active growing of plant crops relying on natural rain, without irrigation.

In such a land use, periods of drought would necessarily be associated with crop failure and reduced land cover, which would increase the wind erodibility of the land surface. We can infer from this observation that the excessive drought in combination to the development of the land to dryland agriculture in this region may lead to most the significant number of dust events. The other two maps also bolster the aforementioned observation, with the total sum and overall mean of drought intensity also highest in the dryland agriculture region around Lubbock, especially to its south and west.

In PART II and PART III of this project, we focused on the time period of 2010-2016 in an area that includes parts of Oklahoma, Texas, New Mexico, Colorado, and Kansas. Although more than 600 dust emission hotspot sites were identified in this area, their potential to produce hazardous blowing dust to affect highway traffic is not equal. Numerous studies have shown that the dust events that deteriorate visibility and therefore jeopardize motorists are associated with preferred land use types that are close to the highway (e.g., Day, 1993; Pauley et al., 1996, Lee et al., 2009). Accordingly, we prioritized the large number of dust emission hotspots to 55 based on their distance to the adjacent highway (i.e., <1 km) and accessibility. Although TSVs and particle-size distribution for soils located at many of these hotspot sites are largely similar, WEPS modeling showed that their potential of blowing dust emission is notably different. Very importantly, in combination with an empirical equation of visibility and particle concentration, we further identified a number of hotspot sites with which close attention must be paid on blowing dust production. Among these hotspots, 8 of them have the highest potential to produce hazardous blowing dust, with the magnitude that could reduce the visibility to < 200 m in certain periods of February and March. The localities of these hotspots illustrated the significance of cropland (in the center region) and shrubland (in the southwestern region) on dust production. In the northern and central study areas, most cropland use is devoted to cotton farming and the local farming techniques leave the soil bare from November to May (Lee et al., 1994; Nordstrom and Hotta, 2004). Lee et al. (1994) also showed that in this period of time strong winds are common and are generally from west and southwest. The location, timing, and magnitude of the dust production at the hotspots are critical information for highway authorities to make informed and timely management decisions when wind events strike.

Dust emission hotspots that are located >1 km away from neighboring highways, although are not specifically investigated in this study, may also contribute hazardous dust to highway traffic. In the southwestern U.S. and many other arid environments in the world, dust plumes that emanate from individual point sources may merge into a large-scale, shield-shaped region of dust (i.e., Darmenova et al., 2005; Miller et al.,

2006; Lee et al. 2009). This large aerosol shield, once passing across a highway, may pose a serious threat to transportation safety.

The rank of the dust emission hotspots to highway safety, however, is not static. Our TSV measurements suggest that dust emission may increase substantially if the soil surface is disturbed or the vegetation cover is lost. This is a particular concern for playas or sites where the physical soil crust may be disturbed by recreational vehicles, cattle grazing and trampling, land use change etc. While TSVs of the hotspot sites were only measured once in our study, they are well-known to vary over time due to changes of soil moisture (Li et al., 2015). Nevertheless, the combination of strong winds and unvegetated, loose sediments in spring and early summer makes these areas highly active hotspots for dust production (Gillette, 1999; Lee et al., 2009; Rivera Rivera et al., 2010). A case in point is the Lordsburg playa, crossed by the Interstate Highway I-10, located near the border of New Mexico and Arizona. Blowing dust has been frequently observed crossing the highway from the surface of the playa (Figure 23) where the soil and vegetation has been disturbed by human activities (Department of the Interior, 1998) and natural flooding events (Scuderi et al., 2010). This blowing dust has caused numerous fatal multi-vehicle traffic accidents on I-10 in recent years, including 10 persons killed in dust-related crashes in 2017 alone (Associated Press, 2017).

Also in southwestern New Mexico, blowing dust has caused road closures and accidents on a mile-long stretch of U.S. 180, about 24 km northwest of Deming. The Department of Transportation of New Mexico has planned to use netting and reseeding to promote vegetation growth on this denuded pasture to reduce hazardous driving conditions created by blowing dust (Associated Press, 2016). Our study identified multiple dust emission hotspots along this highway, and furthermore, the WEPS simulations revealed that this area may be subject to Type II scale of dust events during the time of February and March (Figure 22).

Climate projections suggest that mid-latitude continental interiors of the U.S., including a large portion of the southwestern U.S., will experience warmer and drier conditions (Seager et al., 2007; Diffenbaugh et al., 2008). As a result, soil moisture in summer is projected to be 15-20% lower, and more frequent and persistent droughts are expected (Easterling et al., 1997; Cook et al., 2015). In fact, many of the Great Plains states have experienced multi-year droughts recently (Hoerling et al., 2014) and the impact of the drought on wind erosion has been manifested by the escalated number of dust events observed in 2012 in our study area. Long-term data show that the frequency of dust storms is already increasing (Tong et al., 2017) and the length of the dust storm season is already expanding (Hand et al., 2016) in Southwest North America. A most recent study suggested that projected climate change, along with enhanced land surface bareness, will likely bring more frequent and extreme dust activity to the southern Great Plains in the U.S. (Pu and Ginoux, 2017), and therefore activate some of the low-rank hotspots identified in this study.

Figure 23. A scene of blowing dust passing the highway. Looking east across Lordsburg playa, New Mexico, where Interstate 10 highway crosses a dust hotspot: dust plumes can be seen intersecting the highway on the afternoon of March 22, 2016 (Source: TG). This stretch of road has been the site of multiple vehicle crashes in dusty conditions causing more than 10 fatalities in 2017 alone.

CONCLUSIONS AND RECOMMENDATIONS

A total of 620 dust emission hotspots were identified in the Southern Great Plains and part of the Chihuahuan Desert of the southwestern U.S. from 2010-2016, and these sources primarily occurred on cropland and shrubland, and nearly 1,200 dust emission sources were identified extending back the study period to 2001. Overlaying the distribution of the hotspots and the highway systems, we found that many of these dust sources are located close to highways, therefore could contribute harmful blowing dust to ground transportation. Although TSVs and particle-size distribution for soils located at many of these hotspot sites are largely similar, WEPS modeling showed that the potential of blowing dust emission is notably different, primarily due to land use type. Accordingly, we prioritized the large number of dust emission hotspots to 55 based on their distance to the adjacent highway (i.e., <1 km) and accessibility. Although the WEPS model cannot pinpoint the intensity of individual dust events and the exact timing of their occurrence, results of this study still have important implications for highway authorities to make informed management decisions. Knowing the locations of dust emission hotspots and their potential to produce hazardous blowing dust will also provide a baseline for land managers, as these are the locations where human interventions need to be exercised with the greatest care. These locations may also be especially susceptible to future climate and land use change. Findings of our study represent a first step to ultimately develop an integrated modeling and monitoring system to mitigate the hazardous impacts of dust on highway safety in the U.S. and elsewhere in the world.

IMPLEMENTATION AND TECHNOLOGY TRANSFER

Technology transfer for the proposed project has been focused on reports, conference presentations, and journal papers, as shown in the following list:

Li J et al.(2017), Blowing dust and highway safety in the Southern Plains: Identifying current and potential dust emission “hot spots”, 2017, AAG Annual Meeting (April 5-9), Boston, MA

Lee, J. et al. (2017), Identifying blowing dust sources in Oklahoma, New Mexico and Texas, USA using MODIS imagery, AAG Annual Meeting (April 5-9), Boston, MA

Li J. Atmospheric dust and haze in China and US: A historical perspective on air pollution. Jan 18, 2017, College of Science and Engineering, Oral Roberts University International Forum, Tulsa, OK

Li J (2016), Atmospheric dust: Small-scale processes with global consequences, Department of Geography, Geology, and Planning, Missouri State University, Springfield, MO

Li, J (2015), Atmospheric dust: Small-scale processes with global consequences. Department of Geosciences, The University of Tulsa, Tulsa, OK.

Li, J et al. (2014), Dust and highway safety in the southern plains of the US, AGU Fall Meeting, Dec, San Francisco, CA.

Li, J et al. (2015a), Dust and Highway Safety in the US: Identifying Emission “Hot Spots”, EGU General Assemble, April, Vienna, Austria.

Li, J et al. (2015b), Shifting from grassland to shrubland: New insights from recent studies in the Chihuahuan Deserts. American Geophysical Union Annual Meeting, Dec, San Francisco, CA.

Gill, T. E. (2015) NASA press release, NASA Earth Observatory, September 10, 2015: http://earthobservatory.nasa.gov/IOTD/view.php?id=86571&src=fb, report.

Gill, T. E. (2015), Arizona Dust Storm Workshop, Mar, Casa Grande, AZ.

Journal articles

Li J, Kandakji T, Lee JA, Tatarko JT, Blackwell J, Gill TE, and Collins J. Blowing dust and highway safety in the southwestern United States: Characteristics of dust emission "hotspots" and management implications. Science of the Total Environment, In press.

Li, J and Ravi, S. Interactions among hydrological-aeolian processes and vegetation determine grain-size distribution of sediments in a coppice dune (nebkha) system. Journal of Geophysical Research-Biogeosciences, *in review*.

Li, J., W. P. Gilhooly III, G. S. Okin, and J. Blackwell III (2017), Abiotic processes are insufficient for fertile island development: A 10-year artificial shrub experiment in a desert grassland, *Geophys. Res. Lett.*, 44, doi:10.1002/ 2016GL072068.

Li J, Flagg C, Okin GS, Painter TH, Dintwe K, and Belnap J. On the prediction of threshold friction velocity of wind erosion using soil reflectance spectroscopy. Aeolian Research, 2015, 10.1016/j.aeolian.2015.10.001

REFERENCES

Ashley, W.S., Black, A.W., 2008. Fatalities associated with nonconvective high-wind events in the United States. Journal of Applied Meteorology and Climatology, 47, 717-725.

Associated Press, 2016. “State plans steps to reduce blowing dust on US 180.” Accessed at http://www.lcsun-news.com/story/news/2016/11/29/state-plans-steps-reduce-blowing-dust-us-180/94625100/

Associated Press, 2017. “2 killed in freeway crash in NM dust storm.” Accessed at http://www.lcsun-news.com/story/news/local/2017/02/24/2-killed-freeway-crash-nm-dust-storm/98369206/.

Austin, M.E., 1965. Land resource regions and major land resource areas of the United States (exclusive of Alaska and Hawaii). USDA Agricultural Handbook, 296.

Baddock, M.C., Bullard, J.E., Bryant, R.G., 2009. Dust source identification using MODIS: a comparison of techniques applied to the Lake Eyre Basin, Australia. Remote Sensing of Environment, 113, 1511-1528.

Baddock, M.C., Strong, C.L., Leys, J.F., Heidenreich, S.K., Tews, E.K., McTainsh, G.H., 2014. A visibility and total suspended dust relationship. Atmospheric Environment, 89, 329-336.

Baddock, M.C., Strong, C.L., Murray, P.S., McTainsh, G.H., 2013. Aeolian dust as a transport hazard. Atmospheric Environment, 71: 7-14.

Bullard, J.E., Harrison, S.P., Baddock, M.C., Drake, N., Gill, T.E., McTainsh, G. Sun, Y., 2011. Preferential dust sources: a geomorphological classification designed for use in global dust-cycle models. Journal of Geophysical Research-Earth Surface, 116, F04034, doi: 10.1029/2011JF002061.

Bullard, J.E., Harrison, S.P., Drake, N., Gill, T.E., 2009. Preferential dust sources in global aerosol models: a new classification based on geomorphology. Eos Trans. AGU. 90 (52 supp.), EP23D-01.

Buschiazzo, D.E., Zobeck, T.M., 2008. Validation of WEQ, RWEQ and WEPS wind erosion for different arable land management systems in the Argentinean pampas. Earth Surface Processes and Landform, 33, 1839–1850. http://dx.doi.org/10.1002/esp.1738.

Cook, B.I., Ault, T.R., Smerdon, J.E., 2015. Unprecedented 21st century drought risk in the American Southwest and Central Plains. Science Advances, 1.1. e1400082.

Darmenova, K., Sokolik, I.N., Darmenov, A., 2005. Characterization of east Asian dust outbreaks in the spring of 2001 using ground-based and satellite data. Journal of Geophysical Research 110, D02204. doi:10.1029/2004JD004842.

Day, R.W., 1993. Incidents on interstate highways caused by blowing dust. Journal of Performance of Constructed Facilities, 7(2) 128-132.

Deetz, K., Klose, M., Kirchnerand, I. Cubasch, U., 2016. Numerical simulation of a dust event in northeastern Germany with a new dust emission scheme in COSMO-ART. Atmospheric Environment, 126, 87-97.

Department of the Interior, Bureau of Land Management, NM-030-1220-00. Emergency Closure of the Lordsburg Playa to Off-Highway Vehicles (OHV), Hidalgo County, NM. Federal Register (USA) 63(122), 34661.

Diffenbaugh, N.S., Giorgi, F., Pal, J.S., 2008. Climate change hotspots in the United States, Geophysical Research Letters, 35, L16709.

Easterling, W.E., Hays, C.J., Easterling, M.M., Brandle, J.R., 1997. Modeling the effect

of shelterbelts on maize productivity under climate change: An application of the EPIC model. Agriculture, Ecosystem and Environment, 61, 163-176.
Feng, G., Sharratt, B., 2007. Validation of WEPS for soil and PM10 loss from agricultural fields within the Columbia Plateau of the United States. Earth Surface Processes and Landform, 32, 743–753, http://dx.doi.org/10.1002/esp. i434.
Feng, G., Sharratt, B., 2009. Evaluation of the SWEEP model during high wind on the Columbia Plateau. Earth Surface Processes and Landform, 34, 1461–1468, http://dx.doi.org/10.1002/esp.1818.
G. Wu et al. 2013. Atmospheric dust from a shallow ice core from Tanggula: implications for drought in the central Tibetan Plateau over the past 155 years," Quaternary Science Review, 59, 57–66.
Ganguli, P., Ganguly, A. R., 2016. Space-time trends in U.S. meteorological droughts, Journal of Hydrology- Regional Studies, 8, 235–259.
Gillette, D.A. 1999. A qualitative geophysical explanation for "hotspot" dust emitting source regions, Contributions to Atmospheric Physics (Beiträge zur Physik der Atmosphäre), 72 (1), 67–77.
Ginoux, P., Chin, M., Tegen, I., Prospero, J., Holben, B., Dubovik, O., Lin, S., 2001. Sources and distributions of dust aerosols simulated with the GOCART model. Journal of Geophysical Research, 106(D17), 20255-20273, doi:10.1029/2000JD000053.
Goudie, A.S., 2009. Dust Storms: Recent development. Journal of Environmental Management, 90, 89-94, doi:10.1016/j.jenvman.2008.07.007
Goudie, A.S., 2014. Desert dust and human health disorders, Environment International, 63:101-113.
Goudie, A.S., Middleton, N.J., 1992. The changing frequency of dust storms through time. Climatic Change. 20,197-225.
Goudie, A.S., Middleton, N.J., 2006. Desert dust in the global system. Heidelberg, Germany: Springer-Verlag.
Hagen, L. J., Skidmore, E. L., 1977. Wind erosion and visibility problem, Transactions of the ASAE, 20 (5), 898-903.
Hagen, L.J., 2004. Evaluation of the wind erosion prediction systems (WEPS) erosion submodel on cropland fields. Environmental Modelling and Software, 19, 171–176.
Hand, J.L., White, W.H., Gebhart, K.A., Hyslop, N.P., Gill, T.E., Schichtel, B.A., 2016. Earlier onset of the spring fine dust season in the southwestern United States. Geophysical Research Letters 43(8):4001-4009.
Hoerling, M., Eischeid, J., Kumar, A., Leung, R., Mariotti, A., Mo, K., Schubert, S., and Seager, R., 2014. Causes and predictability of the 2012 Great Plains drought. Bulletin of the American Meteorological Society, 95(2), 269-282.
Lader, G, Raman, A., Davis, J.T., Waters, K., 2017. Blowing dust and dust storms: One of Arizona's most underrated weather hazards, NOAA Technical Memorandum NWS-WR 290.
Laity, J., 2003. Aeolian destabilization along the Mojave River, Mojave Desert, California: linkages among fluvial, groundwater and aeolian systems. Physical Geography, 24,196-221
Lee, J. A., Gill, T.E., Mulligan, K.R., Dominguez, M.A., Perez, A.E., 2009. Land use/ land cover and point sources of the 15 December 2003 dust storm in southwestern North America. Geomorphology, 105,18- 27.
Lee, J.A., Allen, B.L., Peterson, R.E., Gregory, J.M., Moffett, K.E., 1994. Environmental

controls on blowing dust direction at Lubbock, Texas, USA. Earth Surface Processes and Landform, 19, 437–449.
Lee, J.A., Baddock, M.C., Mbuh, M.J., Gill, T.E., 2012. Geomorphic and land cover characteristics of aeolian dust sources in west Texas and eastern New Mexico, USA. Aeolian Research, 3(4), 459- 466, doi:10.1016/j.aeolia.2011.08.001.
Lee, J.A., Gill, T. E., 2015. Multiple causes of wind erosion in the Dust Bowl. Aeolian Research, 19, 15–36.
Lee, J.A., Tchakerian, V.P., 1995. Magnitude and frequency of blowing dust on the Southern High Plains of the United States, 1947–1989. Annals of the Association of American Geographers, 85, 684–693.
Li, J., Flagg, C., Okin, G.S., Painter, T.H., Dintwe, K., Belnap, J., 2015. On the prediction of threshold friction velocity of wind erosion using soil reflectance spectroscopy. Aeolian Research, 19, 129-136
Li, J., Okin, G.S., Herrick, J.E., Belnap, J., Munson, S.M., Miller, M.E., 2010. A simple method to estimate threshold friction velocity of wind erosion in the field. Geophysical Research Letters, 37, L10402, doi:10.1029/2010GL043245.
Li, J., Okin, G.S., Tatarko, J., Webb, N.P., Herrick, J.E., 2014. Increasing consistency of wind erosion assessments across land use and land cover types: a critical analysis. Aeolian Research, 15, 253-260.
Mahowald, N.M., Baker, A.R., Bergametti, G., Brooks, N., Duce, R.A., Jickells, T.D., Kubilay, N.,Prospero, J.M., Tegen, I., 2005. Atmospheric global dust cycle and iron inputs to the ocean. Global Biogeochemical Cycles 19, GB4025. doi:10.1029/2004GB002402.
Marticorena, B., Bergametti, G., 1995. Modeling the atmospheric dust cycle: 1. Design of a soil-derived dust emission scheme, Journal of Geophysics Research, 100, 16,415–16,430.
Middleton, N.J., 2017. Desert dust hazards: A global review. Aeolian Research, 24, 53-63, https://doi.org/10.1016/j.aeolia.2016.12.001.
Miller, S.D., Hawkins, J.D., Lee, T.F., Turk, F.J., Richardson, K., Kuciauskas, A.P., Kent, J., Wade, R., Skupniewicz, C.E., Cornelius, J., O 'Neal, J., Haggerty, P., Sprietzer, K., Legg,G., Henegar, J., Seaton, B., 2006. MODIS provides a satellite focus on Operation Iraqi Freedom. International Journal of Remote Sensing, 27, 1285–1296.
NASS-National Agricultural Statistics Service, U.S. Department of Agriculture, CropScape geospatial portal Available at: http://nassgeodata.gmu.edu/CropScape/, Accessed June 15, 2017.
Nelson, R., Tatarko, J., Ascough II, J.C., 2015. Soil erosion and organic matter variations for central Great Plains cropping systems under residue removal. Trans. ASABE, 58(2), 415-427.
Nordstrom K.F., Hotta, S., 2004. Wind erosion from cropland in the USA: a review of problems solutions and prospects. Geoderma, 121,157-157.
Notaro, M. Yu, Y., Kalashnikova, O. V., 2015, Regime shift in Arabian dust activity, triggered by persistent Fertile Crescent drought, Journal of Geophysical Research, 120 (19), 10,229-10,249.
Novlan, D.J., Hardiman, M., Gill, T.E., 2007. A synoptic climatology of blowing dust events in El Paso, Texas from 1932-2005. Preprints, 16th Conference on Applied Climatology, American Meteorological Society, J3.12.
NRCS, Soil data mart, USDA Natural Resources Conservation Service, Web Soil

Survey, Available online at http://websoilsurvey.nrcs.usda.gov/, Accessed June 20, 2017.
Parajuli, S. P., Yang, Z. L., Kocurek, G., 2014. Mapping erodibility in dust source regions based on geomorphology, meteorology, and remote sensing, Journal of Geophysical Research, 119, 1977-1994, doi:10.1002/2014JF003095.
Park, S. U., Choe, A., Lee, E. H., Park, M. S., Song X., 2010. The Asian dust aerosol model 2 (ADAM2) with the use of normalized difference vegetation index (NDVI) obtained from the Spot4/vegetation data. Theoretical and Applied Climatology, 101, 191-208.
Patterson, E.M., Gillette, D.A., 1977. Measurements of visibility vs mass-concentration for airborne soil particles. Atmospheric Environment, 11, 193-196.
Pauley, P.M., Baker, N.L., Barker, E.H., 1996. An observational study of the “Interstate 5” dust storm case, Bulletin of the American Meteorological Society. 77, 693-720.
Perry, A.H., Symons, L.J., 2002. Highway meteorology, E & FN SPON, pp 208.
Pimental, D., Harvey, C., Resosudarmo, P., Sinclair, K., Kurz, D., McNair, M., Crist, S., Shpritz, L., Fitton, L., Saffouri, R., Blair, R., 1995. Environmental and economic costs of soil erosion and conservation benefits. Science, 267, 1117-1123
Prospero J. M., Lamb, P. J., 2003. African Droughts and Dust Transport to the Caribbean: Climate Change Implications, Science, 302, 1024-1026.
Prospero, J.M., Ginoux, P., Torres, O., Nicholson, S.E., Gill, T.E., 2002. Environmental characterization of global sources of atmospheric soil dust identified with the Nimbus 7 Total Ozone Mapping Spectrometer (TOMS) absorbing aerosol product. Review of Geophysics, 40, 1002, doi:10.1029/2000RG000095, 2002.
Pu, B., Ginoux, P., 2017. Projection of American dustiness in the late 21st century due to climate change. Scientific Reports, 7, 5553, DOI:10.1038/s41598-017-05431-9.
Rivera Rivera, N. R., Gill, T. E., Bleiweiss, M.P., Hand, J.L., 2010. Source characteristics of hazardous Chihuahuan Desert dust outbreaks. Atmospheric Environment, 44, 2457- 2468.
Rivera Rivera, N.I., Gill, T.E. Gebhart, K.A. Hand, J.L., Bleiweiss, M.P., Fitzgerald, R.M., 2009. Wind modeling of Chihuahuan Desert dust outbreaks, Atmospheric Environment, 43, 347- 354.
Scuderi, L.A., Laudadio, C.K., Fawcett, P.J., 2010. Monitoring playa lake inundation in the western United States: Modern analogues to late-Holocene lake level change. Quaternary Research, 73, 48-58.
Seager, R. et al., 2007. Model projections of an imminent transition to a more arid climate in southwestern North America. Science, 316 1181–4.
Sperazza, M., Moore, J.N., Hendrix, M.S., 2004. High-resolution particle size analysis of naturally occurring very fine-grained sediment through laser diffractometry. Journal of Sedimentary Research, 74, 736–743, doi:10.1306/031104740736
Tong, D.Q., Wang, J.X., Gill, T.E., Lei, H., Wang, B., 2017. Intensified dust storm activity and Valley fever infection in the southwestern United States. Geophysical Research Letters 44 (9), 4304-4312.
Wagner, L.E., 2013. A history of wind erosion prediction models in the United States Department of Agriculture: the wind erosion prediction system (WEPS). Aeolian Research, 10, 9–24.

APPENDIX

Characteristics of the dust emission hotspots

Site Number	Longitude (W)	Latitude (N)	County	State	Elevation (m)	Land use/ cover	Sand (%)	Silt (%)	Clay (%)	USDA soil texture	TSV (m/s)	Annual suspension (kg/m2)	Dates of highest erosion	Rank of type of hazard
1	102.5737	32.926	Gaines	TX	999	Cropland	89	9	2	Sand	0.47	12.84	Mar 15-31, Feb 15-29	I
2	102.3938	32.7088	Gaines	TX	999	Cropland	95	4	1	Sand	0.3	12.08	Feb 15-29	I
3	106.1837	31.8076	El Paso	TX	1118	Shrubland	99	1	0	Sand	0.22	11.57	Mar 1-14, Mar 15-31	I
4	102.918	33.6141	Cochran	TX	1146	Cropland	90	9	1	Sand	0.22	9.65	Feb 15-29	I
5	107.7015	32.269	Luna	NM	1356	Cropland	34	55	11	Silty loam	0.25	8.53	April 1-14	I
6	108.4657	31.6603	Hidalgo	NM	1344	Shrubland	9	75	16	Silty loam	0.23	7.52	Mar 15-31, Apr 1-14	I
7	102.6822	34.164	Bailey	TX	1127	Shrubland	96	4	0	Sand	0.32	6.03	Mar 15-31	I
8	101.9128	32.5567	Dawson	TX	905	Cropland	99	1	0	Sand	0.27	5.38	Feb 15-29	I
9	102.3992	33.5905	Hockley	TX	1082	Cropland	52	41	8	Sandy loam	0.54	5.32	Dec 15-31	I
10	102.3999	33.5905	Hockley	TX	1082	Cropland	52	41	8	Sandy loam	0.42	5.32	Feb1-14	I
11	107.7519	32.1089	Luna	NM	1356	Shrubland	88	10	2	Sand	0.4	4.81	Mar 15-31, Apr 1-14	II
12	102.1184	32.3953	Martin	TX	905	Shrubland	89	9	1	Sand	0.3	4.1	Mar 15-31	I
13	106.183	31.807	El Paso	TX	1118	Building_environ	94	5	1	Sand	0.19	4.05	May 1-14	I
14	102.4265	32.3758	Andrews	TX	999	Building_environ	92	7	1	Sand	0.67	3.94	-	II
15	102.7498	33.7909	Cochran	TX	1146	Cropland	44	52	5	Silty loam	0.4	3.79	Feb 15-29	I
16	102.044	33.1667	Lynn	TX	941	Cropland	38	52	10	Silty loam	0.48	3.73	Feb15-29	II
17	101.8136	32.149	Martin	TX	835	Cropland	88	10	2	Sand	0.47	3.32	Feb 1-14	II
18	102.9132	33.589	Cochran	TX	1146	Cropland	92	6	1	Sand	0.3	3.31	Feb 15-29	II
19	101.2556	36.6647	Texas	OK	926	Shrubland	40	54	6	Silty loam	0.46	2.91	Mar 15-31	II
20	107.19	32.2412	Dona Ana	NM	1356	Shrubland	70	27	3	Sandy loam	0.17	2.89	Mar 1-14, Mar 15-31	II
21	102.9165	33.6255	Cochran	TX	1147	Cropland	80	17	3	Loamy sand	0.3	2.81	Feb 15-29	II
22	100.8794	34.2035	Motley	TX	716	Shrubland	55	38	7	Sandy loam	0.37	2.6	Mar 15-31	II
23	101.9548	33.173	Lynn	TX	941	Cropland	39	53	8	Silty loam	0.78	2.55	March 1-14, May 15-31	II
24	107.9073	32.4318	Luna	NM	1356	Shrubland	22	68	11	Silty loam	0.27	2.37	Feb 1-14	II
25	102.3662	33.6472	Hockley	TX	1082	Cropland	31	62	7	Silty loam	0.58	2.35	Feb 1-14	II
26	108.3903	31.764	Hidalgo	NM	1344	Shrubland	85	13	2	Loamy sand	0.3	2.15	Feb 1-14, Apr 1-14	II
27	101.8056	33.2451	Lynn	TX	941	Cropland	83	15	2	Loamy sand	0.38	1.66	Mar 15-31	II
28	101.5809	33.1683	Lynn	TX	941	Cropland	38	54	8	Silty loam	0.81	1.61	Feb 15-29	II
29	102.4369	34.7994	Deaf Smith	TX	1161	Shrubland	35	57	9	Silty loam	0.46	1.07	Nov 1-14	II
30	107.9224	32.4544	Luna	NM	1356	Shrubland	74	23	3	Loamy sand	0.33	1.03	Feb 1-14, Mar 15-31	III
31	103.5982	34.3236	Curry	NM	1402	Shrubland	93	6	1	Sand	0.32	1	Mar 1-14	II

Site Number	Longitude (W)	Latitude (N)	County	State	Elevation (m)	Land use/ cover	Sand (%)	Silt (%)	Clay (%)	USDA soil texture	TSV (m/s)	Annual suspension (kg/m2)	Dates of highest erosion	Rank of type of hazard
32	102.4346	34.8082	Deaf Smith	TX	1161	Cropland	22	67	11	Silty loam	0.47	0.92	Mar 15-31	II
33	102.9165	33.6255	Cochran	TX	1146	Shrubland	80	17	3	Loamy sand	0.4	0.88	Mar 15-31	II
34	107.4354	32.2466	Luna	NM	1356	Shrubland	51	40	9	Silty loam	0.3	0.81	Mar 15-31	II
35	101.9568	33.1668	Lynn	TX	941	Cropland	40	55	5	Silty loam	0.68	0.76	Feb 15-29	II
36	102.61	37.3242	Baca	CO	1395	Shrubland	41	50	9	Silty loam	0.55	0.57	Feb 15-29	III
37	102.842	34.5242	Parmer	TX	1304	Shrubland	60	33	7	Sandy loam	0.33	0.55	Mar 15-31	III
38	103.3726	34.1651	Roosevelt	NM	1219	Shrubland	85	12	3	Loamy sand	0.41	0.52	Mar 15-31	III
39	101.7646	37.3888	Stanton	KS	929	Shrubland	38	54	8	Silty loam	0.51	0.5	Feb 1-14	IV
40	102.4002	38.4548	Kiowa	CO	1295	Cropland	44	51	6	Silty loam	0.54	0.44	Nov 15-30	IV
41	103.3103	34.6473	Curry	NM	1353	Shrubland	63	31	6	Sandy loam	0.47	0.4	Mar 1-14	IV
42	103.3091	34.6411	Curry	NM	1353	Shrubland	69	25	6	Sandy loam	0.65	0.3	Mar 1-14	IV
43	102.9954	34.4229	Parmer	TX	1304	Cropland	72	23	4	Sandy loam	0.47	0.23	Feb 15-29	IV
44	103.0429	38.5048	Kiowa	CO	1279	Cropland	31	59	10	Silty loam	0.49	0.23	Oct 15-30	IV
45	102.6502	34.1989	Bailey	TX	1127	Cropland	91	8	1	Sand	0.41	0.22	Mar 15-31	IV
46	102.9954	34.4229	Parmer	TX	1304	Shrubland	72	23	4	Sandy loam	0.37	0.21	Mar 1-14	IV
47	102.8691	37.352	Baca	CO	1395	Cropland	39	53	8	Silty loam	0.44	0.16	Nov 15-30	IV
48	102.4404	34.7806	Deaf Smith	TX	1161	Cropland	57	35	7	Sandy loam	0.47	0.13	Dec 15-31	IV
49	100.8044	34.0122	Motley	TX	716	Grassland	60	22	18	Sandy loam	0.51	0.07	Nov 1-14	V
50	102.3063	38.0654	Prowers	CO	1033	Cropland	35	31	34	Clay loam	0.65	0.06	Nov 15-30	V
51	101.3992	37.5546	Grant	KS	929	Cropland	83	15	2	Loamy sand	0.32	0.02	May 15-31	V
52	101.0536	36.874	Texas	OK	926	Cropland	33	35	32	Clay loam	0.57	0.02	-	V
53	100.9598	32.8181	Scurry	TX	746	Grassland	34	36	30	Clay loam	0.67	0.02	-	V
54	102.7733	33.8103	Cochran	TX	1146	Cropland	88	10	3	Loamy sand	0.45	<0.01	-	V
55	102.8961	38.4791	Kiowa	CO	1279	Grassland	31	62	7	Silty loam	0.63	<0.01	-	V